

SCUOLA DI SCIENZE

Dipartimento di Chimica Industriale “Toso Montanari”

Corso di Laurea Magistrale in

Chimica Industriale

Classe LM-71 - Scienze e Tecnologie della Chimica Industriale

Synthesis and Characterisation
Of Hydrotalcite-like compounds
for transesterification reaction

Tesi di laurea sperimentale

CANDIDATO

Lucia Frattini

RELATORE

Prof. Fabrizio Cavani

CORRELATORE

Dott.ssa Karen Wilson

Sessione III

Anno Accademico 2012-2013

INDEX

1. Introduction	4
1.1 Bioenergy demand.....	4
1.2 Biomass	6
1.3 Biofuels.....	8
1.3.1 First-generation biofuels	11
1.3.2 Second-generation biofuels.....	12
1.3.3 Third-generation biofuels.....	13
1.3.4 Fourth-generation biofuels.....	15
1.4 Biodiesel and Green Diesel	16
1.5 Transesterification reaction	18
1.6 Heterogeneous catalysis	21
1.6.1 Hydrotalcite-like compound	23
1.6.2 Synthesis of a hydrotalcitic material.....	25
1.6.3 Synthesis of a hydrotalcitic material via alkali-free method.....	26
1.6.4 Templating agent	26
2. Experimental	28
2.1 Catalysis synthesis.....	28
2.1.1 Conventional Hydrotalcite	28
2.1.2 Macro-porouns Hydrotalcite (PS).....	28
2.1.3 Meso-porouns Hydrotalcite (PMMA).....	29
2.2 Material Characterisation	30
2.3 Poly(methyl methacrylate)	30
2.3.1 Poly(methyl methacrylate) synthesis	30
2.3.2 Separation of the polymer for Characterisation	31
2.3.3 Characterisation of the PMMA nano-spheres.....	31
2.4 Transesterification reaction	31
3. Results	
3.1 Catalyst Morphology	33
3.1.1 XRD	33
3.1.2 Porosimetry analyses	36
3.1.3 SEM	37

3.2 Catalyst Composition.....	39
3.2.1 MP-AES and EDX	39
3.3 PMMA Characterisation	41
3.3.2 TGA and SEM.....	42
3.4 HT-PMMA Characterisation.....	44
3.4.1 XRD and EDX.....	44
3.4.2 TGA/DGA, porosimetry analyses, SEM and TEM.....	46
3.5 Catalytic Transesterification	49
3. Results.....	33
3. Results and Discussions	
3.3 PMMA Characterisation	
3.3.1 DLS	41
4. Discussions.....	54
4.1 HT, HT-PS and HT-PMMA characterisations.....	54
4.2 PMMA	55
4.3 Transesterification reaction.....	56
5. Conclusions.....	57
6. Acknowledgements.....	57
7. References	58

Abstract - A series of templated $[\text{Mg}_{(1-x)}\text{Al}_x(\text{OH})_2]^{x+}(\text{CO}_3)_{x/n}^{2-}$ with different structural properties have been synthesised using an alkali-free coprecipitation route. The macroporous materials were obtained using two different kind of templating agents, polymeric materials, in order to cover a bigger size range (750-70 nm). All the materials have been characterized by different techniques: porosimetry, SEM-EDX, TEM-EDX, MP-AES, XRD, CO_2 titration before and after the calcinations process. All the materials have been tested for transesterification reaction of C_4 - C_8 triglycerides with methanol for biodiesel production.

1. INTRODUCTION

1.1 Bioenergy demand

The technology development, driven by an arising scientific knowledge, is carrying out to several environmental problems, such as climatic changing, energy require and toxic gases release, but also to social problems as water and food global supply and population growth. With this scenario, adding the loss of accessible oil fields and the atmospheric CO₂ amount (no more sustainable), are growing up new trends to do research, able to afford climatic, social and economic requires, and new concepts as green chemistry and sustainable production. For that, new non-fossil carbon energy sources have been explored and still must be found; the biofuels are a clear example of it.

To afford this challenge, during the last decade, more and more renewable energies have been promoting and several international agencies have rose their number up, such as the International Energy Agency (IEA) or the OECD (Organisation for Economic Co-operation Development), with the aim to monitoring the international oil market, providing guidelines for the governments to develop eco-friendly and efficient policies. For example, the IEA, founded in 1973 coping the oil crisis, nowadays works to ensure reliable, affordable and clean energy for its 28 Member Countries. Younger is the GBEP (Global BioEnergy Partnership), established in the 2005 by a G8 decision made of 36 partners and 34 observers, which has its Secretariat in Rome, in the FAO head office. In May 2011, GBEP have drafted 24 sustainability indicators to use as guidelines during the production and use of bioenergy. As one of the goals, there is the expansion of bioenergy production, observing the environmental ranges and reaching the CO₂ amount in the atmosphere at 400ppm.

On **Figure 1.**, there are noted the energy use by source in 2009, reported by the IEA in North America:

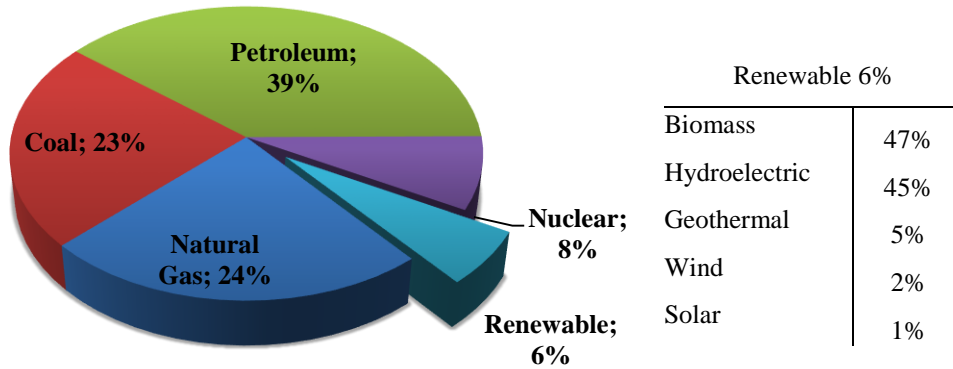


Figure 1: Biomass and US Energy Policy (Biomass Power Association, 2009)

Nowadays the production of bioenergy is a sort of global challenge, the National Renewable Action Plan attributes high hopes to the nearly future of bioenergy; for example, one of the latest Italian goal about bioenergy, is to reach a renewable energy target, considering import and export of 17% in 2020. Nowadays, there are about 15 active plants, for the biofuels production starting from biomass; moreover, in the bioenergetic framework, included most of all transportation, our country needs a real growth about both importation and exportation.

Biomass seems to be a good resource for a plant environmental friendly and with low-emission of greenhouse and toxic gases. Indeed, increasing the amount of feedstock from biomass, displaced to fossil material, it is observed a net reduction of GHG emissions; for example, when it is produced bio-energy from agricultural residues and forestry materials, it is not released methane (CH₄) into the atmosphere, normally obtained by the decomposition of unused material (International Energy Agency, 2007). Consequently, most of the GHG and the toxic gasses emissions depend from technology of bioenergy's production, and from technology of its use; for that reason there are many agencies, as well as the GBEP, focusing their studies also about the entire life-cycle of the emitted gasses.

At the same time using feedstock from biomass may have negative consequences about the land use, as the biodiversity losses and the long-term risk of increasing the GHG emission and degradation of soils and waters. Furthermore, the feedstock supply of renewable materials may involve social and economic conflicts (food markets) and human rights violations.

For example, there are several variables we have to consider designing a plant; one may be its location, meaning not only its access to water and energy power supply, but also in which country it will be located. We often forget that most feedstock, freely from its nature, must be delivered to the plant through the cheapest possible transportation (road, rail or waterway), and there stored easily, in a handy form, better if solid or liquid. The feedstock should be available during all the plant's life, having certified origin and agreeing with the quality demand for environmental duties. Indeed, in order to make competitive bioenergies and so biofuels in the word energy consumption, the biomass production needs to be improved; at the same time, there must be a growth environmental compatible and respect to the land use for food and feeding (IEA Bioenergy, 2011).

The promotion of new technologies and the increasing of the efficiency of biomass integrated plant offer good opportunities to balance the bio-energy production and the socio-economic tasks(IEA Bioenergy, 2012).

Therefore, with this purpose, working with an easy and known technology, the current project tries to improve the biofuels reaction; first of all let start trying to understand what is the meaning of biomass.

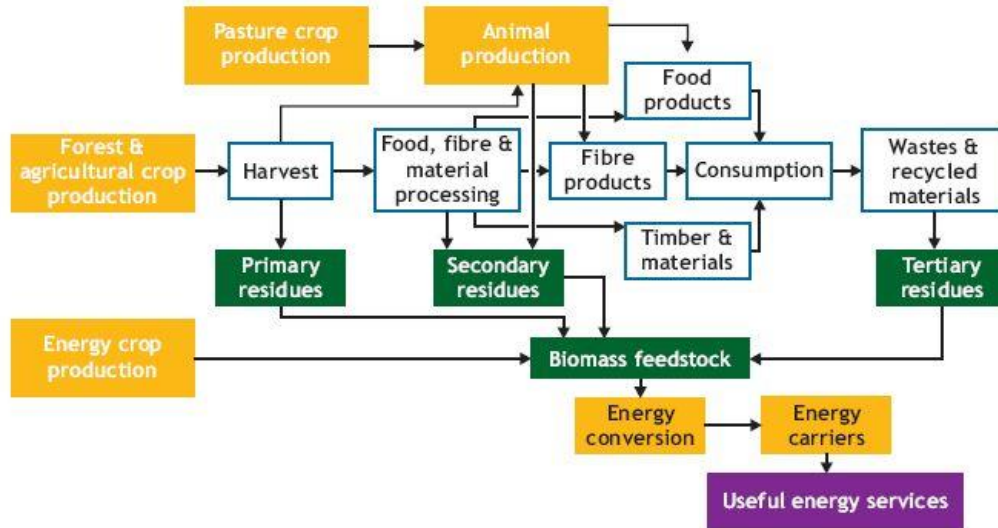
1.2 Biomass

Biomass is a biological material, obtained from organic materials, which can be used to produce renewable energy, as bio-power and biofuels, and bio-products. Focusing our attention on what a biomass is, it must say that at the origin of biomass there is the solar energy, which is stored and converted through biological processes. It is composed of a great variety of agricultural materials (**Scheme 1**: Biomass feedstocks arising from residues and energy crops .), as well as resources from woodland areas, industrial processing residues, and municipal solid and urban wood residues. Different compounds produce primary, secondary or tertiary materials, that gathered, are part of the biomass's matrix:

- The woodland resources collect residues generated in the wood's manufactory and in mills, and forest materials (e.g. dead trees, tree stumps, branches, and wood chips) produced both naturally and during the harvesting.
- The agricultural resources include a wide amount of plants such as: grains, bamboo, hemp, corn, sugarcane, and a great variety of trees, vegetable residues

from crops, such as cotton, sugarcane, rice and fruit; animal manures, and little crop residues from corn and small grains as wheat straw.

- Municipal and urban wood residues include a variety of construction materials, yard materials and packaging materials, furthermore food waste(Perlack, et al., 2005).



Scheme 1: Biomass feedstocks arising from residues and energy crops (International Energy Agency, 2007).

Biomass can be used producing bioenergy, in the small and large scale; therefore, if in small scale it may be possible save on energy bills, for supplying heat, for private houses, or individual buildings such as school, hospitals, animal buildings or greenhouses on a farm or in a village. With a larger scale, in a bioenergy plant, the produced power can provide on-site heat as process heat, district heat, and electricity or feed the national grid. Designing a bioenergy plant, usually, it carries on scale strategies and economies; these are often constrained by the additional transport costs; even it may be necessary to collect the biomass from larger distances, increasing its cost. One example are wood pellets from Canada, already travelling to the market in Scandinavia for heating plants, and palm oil from Malaysia direct in Sweden and the Netherlands for biodiesel feedstock (International Energy Agency, 2007). In the last decade, more and more companies, all around the world, are grounding their market on biomass production, to obtain bio-energy and bio-products. Nowadays, one goal of the bioenergy producers, is to get more biomass than the one available in standard conditions; in southern China, for example, it

is developed a multi-level culture of rubber trees, tea and pepper plants, or like in Brazil with Eucalyptus, grass and dairy cows, or production of winter feed for cattle on sugarcane land. Others solutions are possible, such as the growth of new species finalized to produce energy, with short rotation times. The IEA have identified three important guidelines, to follow producing energy crops:

- crops, harvesting and storage as much economic as possible;
- most appropriate species relatively to the soils and climatic condition;
- maximum use of old instrumentation and rotation's times management minimising the consequences of new aspects.

Furthermore, there are some specific biomass feedstocks, such as oilseeds in the biodiesel production or sugar and starch in the bioethanol production, which need water, nutrients and other cares for their growth. We have to value all of these conditions, avoiding, as said, any sort of competition with the food supply; for example, harvests of corn for bioethanol production need to a big amount of fertilisers, nitrogenous based, and chemicals, which added to fossil fuel feeding, make a controversial process.

However, three different criteria of biomass's characterisation are identified:

- water amount (dry or wet);
- its origin (vegetable or animal);
- living beings contents;

Without forgetting that there are different branches where biomass can be used either directly or after working steps; studying lignocellulose's amount is developed a wide range of biofuels. Here the term biomass will be referred to biobased fuels production, in the liquid phase, finalized for the private and public transportation. Depending by the biomass source, indeed, and by the process used, are obtained biofuels of first and second generation. For example, bioalcohols, biodiesel and green diesel are concerned to the first-generation class and biofuels from sustainable feedstock as second-generation one. Thus may be important remember what is a biofuel and which are its different categories developed through years.

1.3 Biofuels

A biofuel is a fuel made from biomass conversion through different pathways: chemical, biochemical and thermal(Melero, et al., 2009).

Remembering what a petroleum fuel is, will be easier understand the nature of biofuels. Therefore, a fuel is a sort of energy vessel, from which we are able to get power; the carbon fixation is the process to obtain organic compounds from inorganic carbons (like CO₂ during the photosynthesis of plants). Both biofuel and fossil fuel are hydrocarbon chains and they depend from organic materials; the two processes are different in the time their reaction takes place. Fossil fuels are produced with long formation period, approximately in millions of years, causing their not renewability; biofuels are considered renewable by the biomass growth time, that needs years or even shorter. Most important, it is necessary remember the different between renewability and green energy; due that, even if biofuels are renewable, they cannot be considered green. When we define energy as green, it means that its use is not harmful for the ecosystem, and there are no environmental consequences, such as the solar energy. Therefore, producing greenhouse gasses during their use, biofuels are not considerable green; we can assume that all green energies are renewable, but the opposite is not always true.

Generally, biofuels use is restricted to transportation even if they can potentially be used in every sector of application. One of the reasons why biofuels are used as fuels for vehicles is their easy handling; that is true not only during the engine work of pumping but also during their storage. In addition, they can be used as replaced of fossil fuels, with some possible addition for fluid dynamic's problems. Moreover, the chemistry of biofuels is nearby to fossil fuels ones; an example of it is their structure which that show a similar behaviour. A short comparison is reported in the **Table 1** here below, where are compared bio and fossil fuels depending on their chemical structure and their application.

Biofuel	Fossil Fuel	Differences
Ethanol	Gasoline/Ethane	The using of ethanol in gasoline engines, are needs modification. Briefly, ethanol has cleaner combustion products, even if produces more ozone than gasoline. Ethanol has energetic values double considering the ones of gasoline.
Biodiesel	Diesel	They are energetically the same, however biodiesel burned products are cleaner and have a lower particulate and sulphur

		amount. It is more corrosive than ULSD diesel; that obligates a proper technology for the biodiesel engine.
Methanol	Methane	Methanol, compared to methane, has energetically one third of half of its power yield. The transportation of methanol, as liquid, is easier than the one of methane, as a gas.
Biobutanol	Gasoline/Butane	Biobutanol has slightly less energy than gasoline, but can run in any car that uses gasoline without the need for modification to engine components.

Table 1: Biofuels versus Fossil Fuels (Biofuel.org, 2010).

As reported on the table, biobutanol seems have good properties, comparing the advantage using the same engine and the energetic yield; not such as methanol, that, shows storing's convenience, but at the same time, it produces low power to be considered a fuels and not an additive. Biodiesel, even if it is cleaner than petroleum diesel, needs a proper technology; ethanol in its condition, is not enough clean, even its yield is twice than gasoline.

As said, most of biofuels are derived from biomass or biowaste, both from animal or vegetable origins; in theory, any carbon source may feed a biofuel plant, what it is different is how much it is easier convert the biomass to the liquid fuel. For example, different types of biofuels are obtained depending from the feedstock kind: on one hand, it is needed the collection of raw materials, which produce usable diesel oil only after fermentation process (chemical or biochemical process). On the other hand, there are plants, as jatropha and algae, which or produce an oil which replaces directly the diesel oil, after heating treatment (physical process), or to use as starting materials for the biodiesel formation reaction.

The feedstock's nature is a balance between agricultural markets on-site of production and transportation costs; for that reason, the pant's designers choose what better fits their expectations. Some examples are switchgrass, soybeans and corn in the United States,

sugar cane in Brazil, sugar beet and wheat while in Europe, south-east Asia produces miscanthus and palm oil while India produces jatropha.

As we said, different biofuels types are individuated depending from their nature and from process in which they are involved. Therefore, first, second, third and fourth generation of biofuels are developed.

1.3.1 First-generation biofuels

In this category, there are involved: ethanol and bioalcohols, biodiesel, green diesel, bioethers, biofuel gasoline, biogas, syngas and solid biofuels.

Biofuels of first generation are the ones produced from starch, sugar, vegetable oils and animal fats, most of the crops for food; due of that, their use is not view highly. An example of that are corn crops, one of the most important sources in the ethanol manufacturing in the U.S., and at the same time, a primary material for the food world supply. What has fascinated researchers and most of all industrialists using corn crops, is the possibility to use the entire plant to produce ethanol as well, and the already infrastructures for its managing. Sugar cane has similar problems; even if yield in ethanol production is higher and rather than the one starting by corn, only Brazil and some other few countries have adopted this market policy. Vegetable oil, as we said, can be or easily converted in biodiesel or used in diesel engine with additives (to avoid the formation of conglomerates). However, the possible consequences on environmental biodiversity are the most important cause to reduce their using. Although the number of disadvantages, researchers are trying to minimise their competition with food and increase the efficiency of reaction in which they are involved.

We summarize the first-generation biofuels in the **Table 2** below:

Fuel	FeedStock	Energy Density (megaJ/kg)	Greenhouse Gas - CO2 (kg/kg)	Notes
Bioalcohol	Starches from			
Ethanol	wheat, corn,	30	1,91	
Propanol	sugar cane and	34	N/A	
Butanol	fruits	36,6	2,37	
Biodiesel	Oils and fats including animal fats, vegetable oils and algae	37,8	2,85	
Green Diesel	Made from hydrocracking oil and fat feedstock	48,1	3,4	The same chemistry of fossil fuel diesel

Vegetable Oil				
Sunflower Oil	Unmodified or	40	2,8	
Olive Oil	slightly modified	39	2,8	
Fat		32	N/A	
			2,74	
Biogas				
	Methane produced from waste through anaerobic digestion or bacteria			The direct effect of methane is not considered. It is 23x more as effective as a GHG than CO2
Bioethers				
	Dehydration of alcohols	N/A	N/A	As additives to other fuels, increase performance and decrease ozone emissions,
Solid Biofuels				
Wood	Everything from wood and	16-21	1,9	This category includes a very wide variety of materials.
Dried plants	sawdust to	10-16	1,8	
Bagasse	garbage,	10	1,3	
Seeds	agricultural waste, manure	15	N/A	

Table 2: General trends of biofuels of first generation(Biofuel.org, 2010)

Table 2 shows most of all the component of first-generation biofuels, from which primary materials, they are produced and what is their application. Additionally, there are reported also some important component, such as the amount GHG emission (kg)/referring to kg of burned mass and the energy density, reported as (mJ/kg); rapidly, it is possible notice that: biodiesel is the one with higher energy density. Therefore, the potential energy which is obtainable during the burning process, is high; at the same time it produces also the higher amount of GHG.

With this scenario a new approach was needed, and so grew up the second-generation biofuels.

1.3.2 Second generation biofuels

Biofuels of second generation, also named advanced biofuels, differ from the first generation ones by the primary materials; indeed, while the formation process of first generation biofuel is supported by a well known technology; for biofuel of second generation, the changing the chemical structure of feedstock, as the lignocelluloses amount, change also its technology. Working with second-generation feedstock, it has developed a technology known, but less used in this field:

Thermo-treatment:

- gasification: carried out under a controlled oxygen (or steam) flow at 700°C; its products are CO, CO₂ and H₂ (syngas) and it is slightly different to combustion, that is a complete oxidation reaction;
- pyrolysis: it is a thermo-decomposition process, carried out in absence of oxygen, irreversible and its final step is the carbonisation;
- torrefaction: it is an intermediate step, similar to pyrolysis but carried out at lower temperature; usually it is used making easier the biomass transportation and increase the yield on fuels during the following step as gasification or pyrolysis.

Biochemical treatment:

Biochemical treatment involves biological and chemical processes, which convert urban waste and other primary materials by fermentation using genetically modified bacteria.

Avoiding competition with food suppliers, there are not moral and social problems; furthermore, food crops can be a second generation feedstock, only when they are no more good for human supply. Examples of those resources are: grasses (switchgrass, miscanthus, indiangrass), jatropha and seeds crops, waste vegetable oil (WVO) and solid waste.

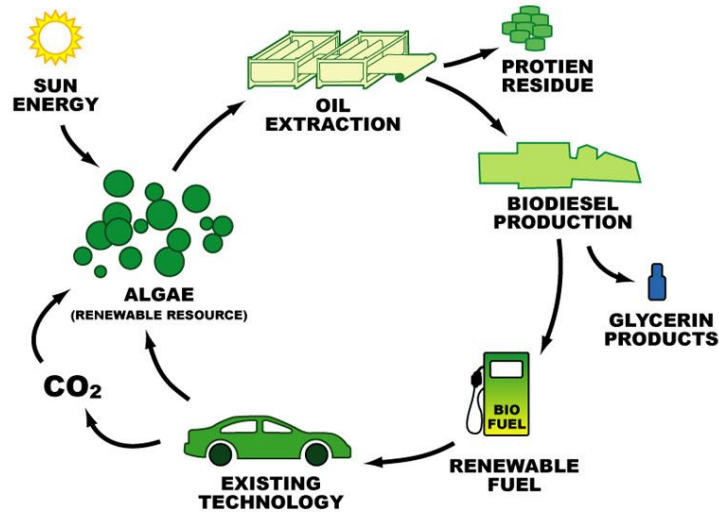
Considering the capacity of grasses producing energy, they have a yield extremely high, about 540%; furthermore, they grow on marginal land, in short time, with a low amount of fertilizers. Unfortunately, there are several disadvantages that make them fewer useful, such as water need, climatic conditions less arid as possible, harvest's density difficult to reach with grasses.

Another resource of the biofuels of second generation is jatropha, which in these last few years is becoming rather popular increasing its market, as well as camelina, oil palm and rapeseed, whose seeds have a high yield to oil, more than soybean. Nevertheless, one of the best options is the WVO, because they are already available, they can be used in diesel engine, but they need to be properly refined avoiding agglomeration and damaging.

1.3.3 Third generation biofuels

This third generation biofuels was been created considering the biofuels production only from algae. Algae are organisms able to create organic matter from inorganic materials and energy, not obtained through nutrition, such as solar energy which is converted to

chemical energy through photosynthesis reaction. Organisms likewise are defined autotrophs (producer or self-feeding), and 50% of their weight is oil, that make them a great feedstock in biofuels manufacturing. **Scheme 2:** explains easily the production chain starting from algae:



Scheme 2: Production chain using algae as feedstock

The algae's importance is due to possibility of :

I case: physic extraction of the oil from vegetable matter, and then, after refining process, we can obtain or a diesel or a gasoline components, depending of species.

II case: it is possible obtain directly biodiesel, bioethanol, biobuthanol and gasoline, modifying genetically the algae. Most of all, yields in oils are higher than the ones obtained with second generation biofuels:

Moreover, algae can grow in most of different conditions, both climatic and of waters; in order to have an industrial production of feeds to stock, what is important, is a massive amount CO₂; indeed, during their photosynthesis process, helped by light, algae fix carbon dioxide into sugar (Gao, et al., 2012).

On **Table 3** are reported some yield values of oils obtained in the first case by second-generation catalyst, such as soybean, sunflower and coconut (castor oil plant, is a plant derived from ricin's family), on the other hand there are algae oils. The table is useful to face the large amount of oils produced with a hectare of algae, almost 26 417 gallons, against the higher amount obtained from Palm plant: 1 572 gallons.

Yield of various plant oils (Gallons per hectare)

BIOFUEL	GENERATION	SECOND-		
			Soy	118
			Sunflower	206
			Castor	373
			Coconut	605
			Palm	1'572
BIOFUEL	TION	THIRD-		
			Algae	26'417

Table 3: Oil amount obtained by feedstock hectare. A gallon is approximately 4 litres. Open source (Bell, 2008).

Therefore, one of the best benefits of algae's use is their consumption of direct amount CO₂; that turn the attention to the fact that, this large CO₂ amount can become a problem. Consequently, researchers are planning to integrate algae cultivation to fuel plants, in order to limit CO₂ and the other GHG emissions and permit a direct source of co₂ to the marine plants. Another drawback to using algae is their high nutritional's cost, such as nitrogen, sulphur and water; adding all of those fertilisers it is increased so much the algae biofuel's value that few years ago, companies have shelved their cultivation (Wijffels & Barbosa, 2010).

1.3.4 Fourth generation biofuels

Biofuels of fourth generation are produced from biomass as feedstock, with the task to have a starting material as more sustainable as possible, which is not far from biofuels of second and third generation. What is new, is the formation process of biofuel; therefore, the plant is integrated, into each step of production, with a capture system of CO₂. A capture system involves for example an oxyfuel combustion, which converts gas flow in carbon dioxide and water, using pure oxygen; after that the produced CO₂ is stored into a undergrounded deposit, which can have natural origins or not, such as a geological basin. The result is a negative carbon dioxide emission during the entire process; moreover, it is possible reduce the CO₂ atmospheric amount, not only limiting its emission, but also removing it from the atmosphere. This integrated plants, called BECCS (Bio-Energy Carbon Capture and Storage), are still not developed in the world market; some

researcher have pointed out that the technology and materials in a CCS plant can produce dangerous waste, and that they are not energetically convenient (Wilson, et al., 2007). Additionally, some opponents argue that there could be the possibility of environmental changes and catastrophic consequences, a slow release of the stored gasses, and at the same time a too fast release (Riahi, et al., 2004). The carbon sequestration and storage, even if it is not a new technology, has still long time until its application will be consolidated. At the time, the only chance we have, is integrate BECCS with some other bioenergy plant, in order to develop a sort of cooperation between bioenergy processes.

1.4 Biodiesel and Green Diesel

Biodiesel and green diesel are fuels obtained or from feed stocks containing triglycerides with different chains length as animal fats and vegetable oils (biodiesel and green diesel); or from sugars and starch such as bioethanol (NREL, 2003).

However biodiesel is a nonpetroleum-based fuel that consists of a mixture of fatty acid alkyl esters (FAAEs) obtained or from transesterification reactions of triglycerides (TGs) or from esterification of free fatty acids (FFAs), both drive with low molecular weight alcohols as, for example, methanol or ethanol (Loterio, et al., 2005). Each triglyceride is composed of three chain fatty acid of a variable number of carbon atoms, with different length, unsaturation degree and branching. These differences influence directly the physical and chemical characteristics of the biodiesel, and are strictly related to the feedstock composition used. Therefore, for example, the unsaturation degree of the alkyl chain changes the fuel's density and its viscosity, affecting its behaviour under temperature fluctuation. If a material, likewise biodiesel, doesn't keep its characteristics as constants, with the temperature's modulation, properties can change, as well the enthalpy or the heat capacity, which both increase, to a rising of temperature (Klemes, et al., 2011). Other variable properties define material's physical and chemistry during their using, such as the behaviour under cooler condition, or their ignition delay.

The Iodine Value (IV) is one of the most commonly applied indices in fatty acid chemistry and it is used to compare the number of unsaturations (C=C) contained in natural complex mixtures of fatty acid alkyl esters; common IV of second generation diesel are reported on Table 4: Table of Iodine Values

Fat

Iodine Value (IV)

Palm oil	44-51
Olive oil	80-88
Coconut oil	7-10
Sunflower oil	125-144
Soybean oil	120-136
Peanut oil	84-104

Table 4: Table of Iodine Values

Its evaluation is a iodometric analysis, by which it is related Iodine mass (g) that it is consumed by 100 grams of a chemical substance, as in that case fat. Generally, the fatty acid solution is treated with an excess of a solution of glacial acetic acid, containing ICl (iodine chloride) or IBr (iodine bromide); the iodine reacts on one hand with fatty acid's unsaturations, on the other hand with, the excess, reacts with KI (potassium iodide), forming the iodine. It is possible quantify the concentration of iodine in the solution, by titration with sodium thiosulfate.

However, an higher iodine value means an higher number of double bonds in the biofuel, low saturation degreesuch as the sunflower oil and soybean oil. At this condition it is higher the possibility to have deposit into engine, due actually, to unsaturated bond.

Normally, biodiesel needs low iodine value, so a high saturation degree(less C=C); what's more is that lowering of IV promotes a higher Centane Number(CN), for which the inition delay is shorter (Rao, et al., 2010). Briefly, the CN is a parameter to estimate the quality of diesel during its ignition through compression; furthermore, it quantifies the ignition delay, or rather, the time between starting and volume's first sensible expansion (during which it is shown a rise of pressure). As much higher is the cetane number, easier will be the compression ignition; at the same time, better will the diesel engine work . Nowadays in European Union, the CN values range is from 46 to 51,otherwise in North America it is set in the 42-45 range, even if higher CN are possible. The Cooperative Fuel Research (CFR) engine is been commissioned of the measuring of its value, under standard condition; in order to increase the CN value it is possible use additives such as alkyl nitrates or di-tert-butyl peroxide. There are other parameters useful to characterise a diesel, such as diesel's lubricity, density, and its cold-flow properties and sulphur content. However, using additives, to improve the flow properties of the biodiesel at low temperature, has been proposed to solve the problem, at

least in part. Causing its density property, about 9% less dense energetically from the petroleum diesel, it cannot be used in the current diesel engine, fuel lines or other rubber components. Moreover considering the high costs of reagents (methanol included), Eni S.p.A. and UOP LLC have been started a collaboration, simplifying the synthesis process, in order to develop a new product: green diesel. The collaboration result is Ecofining process, from which it is obtained green diesel. What is revolutionary of green diesel is: although having the same properties of a petroleum diesel that allow it to be used in the existing diesel engine, at the same time, it is named green, for the sulphur content and its feedstock.

To have just a view, on **Table 5:**, there is a comparison between the different properties of diesel oil obtained through different synthesis method:

	Ultra Low Sulfur Diesel (ULSD)	Biodiesel (FAME)	Green Diesel
Oxygen Content (%)	0	11	0
Specific gravity	0,84	0,88	0,78
Sulfur content (ppm)	<10	<1	<1
Heating Value (MJkg ⁻¹)	43	38	44
Cloud Point (°C)	0	-5 to 15	-20 to 20
Distillation Range (°C)	200-360	340-370	200-320
Polyaromatics (wt%)	11	0	0
NOx emission (wt%)	Baseline	+10%	-10%
Cetane Number (CN)	51	50/60	70/90
Stability	Baseline	Poor	Baseline

Table 5: Comparison between Green diesel, ULSD and FAME (Cavani, et al., 2009)

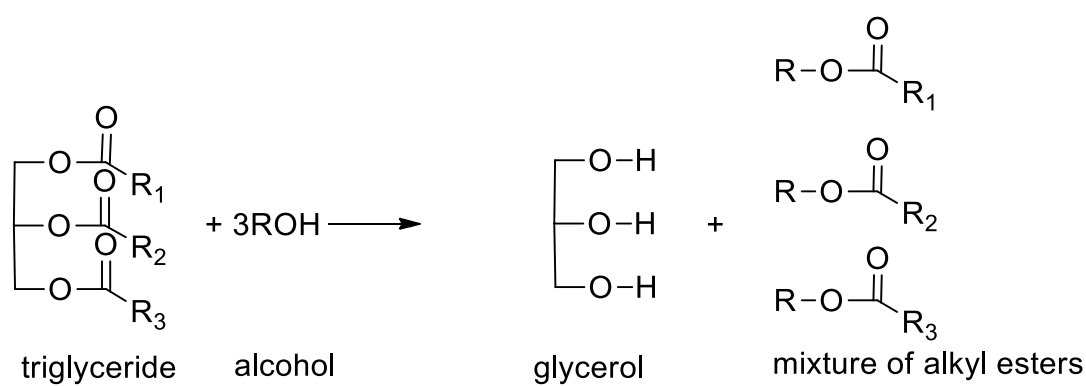
As said in the last paragraph, the sulphur content of the new generation diesel is lower than the traditional diesel, even if desulfurated; additionally, the properties of the fuel, density and viscosity, may influence the spray efficiency of injection, so that, produce a different amount of NOx into exhaust.

1.5 Transesterification reaction

In the present work, it is achieved the biodiesel synthesis via transesterification reaction with heterogeneous catalysis; tests have been carried out on triglyceride with short chain

in order to verify the efficiency of the catalyst, hydrotalcite-like compound, for which it has been tried to create a ordered structure.

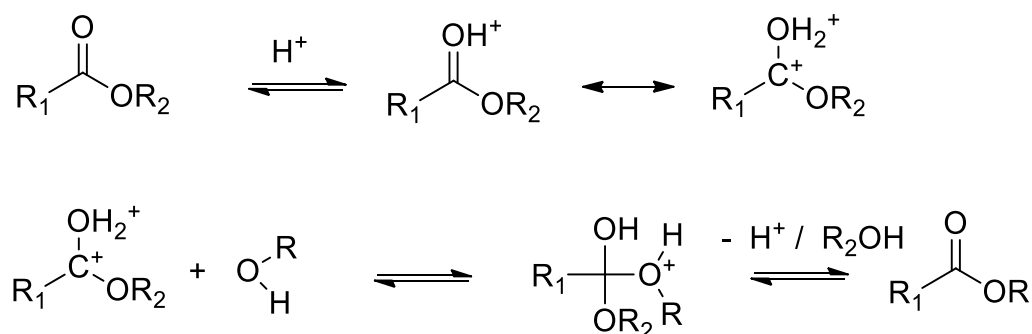
A transesterification reaction is an equilibrium reaction and, even if transformation occurs by mixing the reactants, the presence of a catalyst (strong acid or base) increases the reaction rate up to the equilibrium. Usually when the triglyceride reacts with the alcohol, the produced mixture is made of fatty acid alkyl esters (mono- and diglyceride) and alkyl esters, triglyceride unreacted and glycerol. The transesterification processes indeed stepwise, during which, first the di- and second the monoglycerides, are formed as intermediates.



Scheme 3: Transesterification reaction.

The transesterification reaction can be carried out in acid or base catalytic condition, in absence of water, in order to avoid the competitive formation of the carboxylic acids that reduces the yield of the alkyl esters, and with an excess of the alcohol to increase the same. The firsts catalytic developed processes works in homogeneous phase following different pathway in the mechanism, depending with the acidity or basicity of the catalyst.

The acid-catalyzed mechanism tranesterification occurs starting with the protonation of the carbonyl group of the ester leading a primary carbocation with a low electron density. This condition allows an easy attack by the alcohol to the C⁺ forming a tetrahedric intermediate. After elimination of glycerol, the catalyst is regenerated and the new ester released.



R: alkyl group of the alcohol

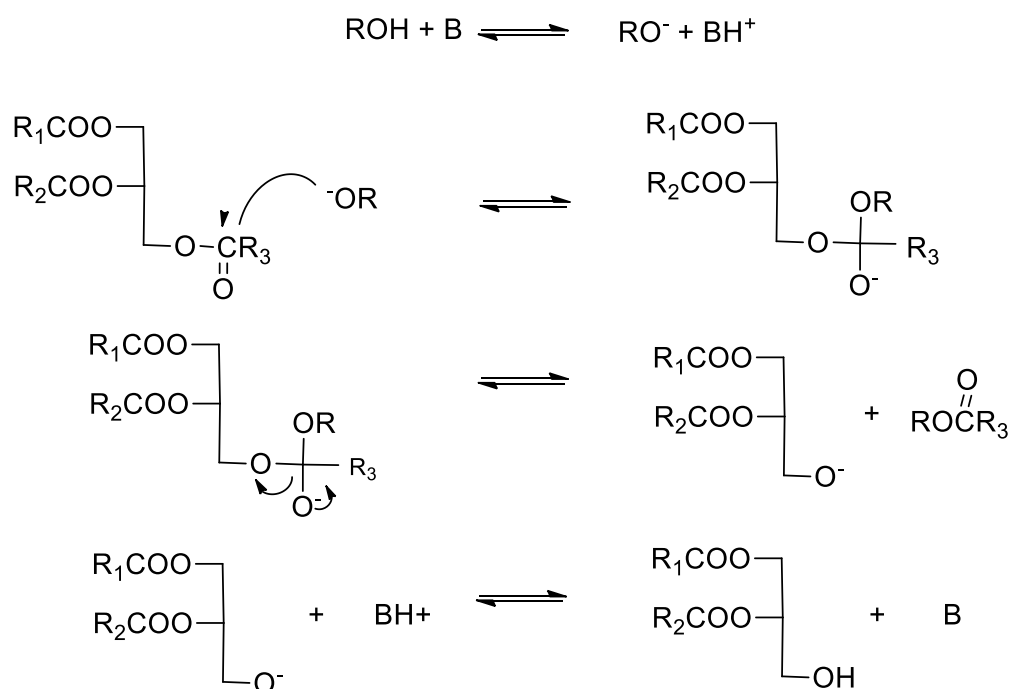
R1: carbon chain of the fatty acid

R2: glyceride $\begin{array}{l} \text{---O---} \\ | \\ \text{---O---H} \\ | \\ \text{---O---H} \end{array}$

Scheme 4 Transesterification reaction in an acid-catalyzed mechanism.

A base-catalyzed process operates with a transesterification mechanism, faster than the acid one, and for that is the most used in an industrial level.

The reaction occurs starting with the protonation of the catalyst and the formation of an alkoxide, which attacks the carbonyl group of the triglyceride, generating a tetrahedral intermediate from this the diglyceride and the alkyl ester are formed.



Scheme 5: Transesterification reaction in a base-catalysed mechanism.

Alkaline metal alkoxides (as CH_3ONa) give high yields (>98%) in short reaction time (30min); even if they carry out to good results, working with them means work in total anhydrous condition, aim difficult to reach when they speak with industrial terms. Due to this reason, a good alternative are the alkaline metal hydroxides as KOH and NaOH; those are less active than alkoxides and the problem can be overcome increasing the catalyst amount (Schuchardt, et al., 1998).

Homogeneous catalysis, and mainly the base catalysts, have several problems during their removal, caused by the formation of stable emulsion and saponification reaction. During a saponification reaction occurs the hydrolysis of the fatty alkyl ester with the alkaline metal hydroxide, forming the alkylic carboxylate salt, doing difficult the separation of the methyl ester.

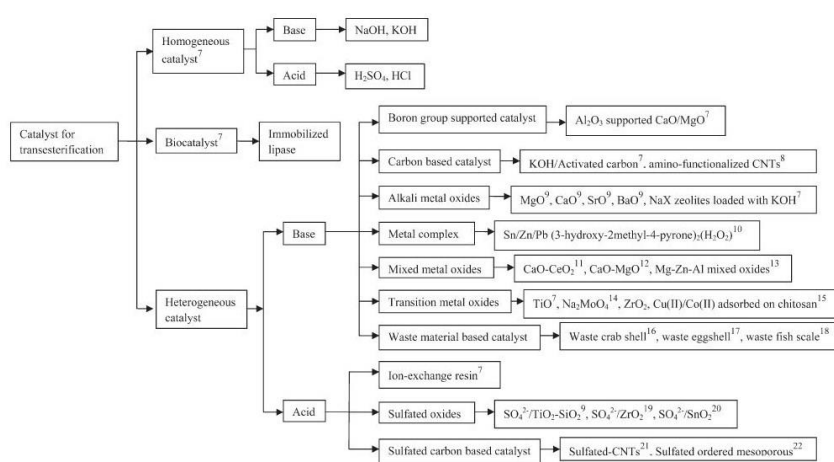


Figure 2: Classification of catalysts used in transesterification reaction (Shuit, et al., 2013)

A transesterification process, with a heterogeneous catalytic system, offers, not only all the advantages that a solid catalyst can carry out, such as the easily to separate all the components, reducing capital and energy costs. Furthermore, it can be a new green technology, making the catalyst reusable, with a minimal aqueous waste, a minimal saponification reaction risk and not neutralization of products.

1.6 Heterogeneous catalysis

Briefly, heterogeneous catalysis, at industrial scale, can be preferable than the homogeneous catalysis since, as we said, separation and collection of products, unreacted materials and catalyst are easier to design, such as in the plant itself reducing the steps number or making it continuous. Moreover, purity is improved and corrosion's problems

reduced. Generally it is possible to define a catalyst in heterogeneous form depending on their chemical behaviour: the more known redox, acid-based or poly-functionalised, and the new branch of enzymatic chemistry or with catalyst soluble in ionic liquid.

Unfortunately, there are disadvantages with heterogeneous catalytic reaction, such as that occurs by a sequence of elementary steps that includes:

- Adsorption;
- Surface diffusion;
- Chemical rearrangements, such as the bond breaking, bond forming and molecular readjustment of the adsorbed intermediates;
- Desorption of the products.

All these problems, due to physical and chemical boundaries, linked to mass transfer and diffusion between catalyst and the environmental condition, define the global rate of the reaction. If in the liquid state there are two phases, the diffusion step of the reagents in the pore of the catalyst is limited and the availability of the active sites for the catalytic reaction is reduced, decreasing the reaction rate (Somorjai, 1994). Changing only its morphology or the component nature, it is possible to promote one step, reducing rate, but also using promoters. The catalyst's nature can be widely different, depending if it is supported or not; for example, a heterogeneous catalyst can be supported, as in the case of a catalyst existing, or be support of itself. There can be physical promoters and chemical promoters that help through different ways catalyst activity; on one hand, physical promoters are used to stabilise the surface, on the other hand chemical promoters help activity and selectivity.

However, in a heterogeneous catalytic process, the transesterification reaction faces, for example, mass transfer resistance problems due to a three-phase system (triglycerides, alcohol and solid catalyst). These conditions reduce pore diffusion rate and deactivate the catalytic sites, useful for the reaction. Moreover, leaching of the active species and fouling of the catalyst surface by organic substances in the reaction media have been identified as the main factors in catalysts deactivation. To minimize the mass transfer limitation and to increase the yield of biodiesel, the proper configuration design of catalysts and their operating conditions are required. Structured solid may be an attractive solution of the problem; well-defined catalyst can operate better than a non-ordered solid. Silica mesoporous supporting organic active species is one example of several, for which homogeneous catalyst has been "heterogenized". Periodic Mesoporous

Organosilicas (PMO) are materials containing pores with diameters between 2 and 50nm. Porous materials are classified into several kinds by their size. According to IUPAC notation, *microporous* materials have pore diameters of less than 2nm and *macroporous* materials have pore diameters of greater than 50 nm; the *mesoporous* category thus lies in the middle. A PMO consists of a sequence of alternating hydrophilic silanol groups (Si-OH) and more hydrophobic organic parts. It is possible incorporate a wide variety of compounds into channel's wall. Choosing carefully their organic precursors, bridging units could be ethane, ethene, benzene, biphenyl, or thiophene, and also functional groups such as amino and sulfonic acid.(Mizoshita, et al., 2011). Furthermore, PMO materials have an arrangement of pores ordered, which have a sharp size distribution, designed by employing during the synthesis of structure-directing agent, also called templating agent. PMO synthesis, usually, is carried out in acid condition, using non-ionic surfactants. By controlling the nature of the organic segment, the type of surfactant and the formation conditions, one can control the physical and chemical properties of the resulting PMO and produce highly ordered porous structures with a periodicity on the nanometer scale (Morell, et al., 2006).

In the present work has been studied the transformation of triglyceride C4 and C8 with methanol as low weight molecular alcohol, in presence of an hydrotalcite-like compounds as solid catalyst. The reached goal is the same seen using PMO as catalyst, or better have a heterogeneous catalyst, sufficiently active with an ordered structure to promote reaction, reducing the leaching and poisoning of surface.

1.6.1 Hydrotalcite and Hydrotalcite-like compound

Hydratalcite is a natural mineral, anionic clay, double layered, and based on Mg^{2+} and Al^{3+} ions and hydroxide; due its structure, a hydrotalcite is a particular branch of the Layered Double Hydroxides (LDH) materials; its general formula is $Mg_6Al_2(OH)_{16}CO_3 \cdot 4H_2O$ and its structure is similar to $Mg(OH)_2$ /brucite.

Consequently, Hydrotalcite-like compounds(HTlc) are a layered double hydroxide, belonging to the class of the anionic clays, with the general formula $[M^{II}_{(1-x)}M^{III}_x(OH)_2]^{x+}(A^{n-})_{x/n} \cdot zH_2O$. M^{II} and M^{III} are respectively divalent metal cations, as Mg^{2+} , Ni^{2+} , CO_2^+ , Zn^{2+} , Cu^{2+} , and trivalent metal cations (e.g. Al^{3+} , Fe^{3+} , Cr^{3+}) that occupy octahedral positions. The subscript x is the atomic ratio of the $M^{III}/(M^{II} + M^{III})$, A^{n-} is the interlayer anion and z is the number of interlayer water molecules. The nature

of the anion has no limitation, and it is possible to intercalate first simple compounds by a coprecipitation method and then incorporate others anions by anion exchange (Hibino & Tsunashima, 1997). The structure is defined by octahedral coordinations, where OH⁻ groups of both metals, occupy a shared edge and build the entire structure as a double layers. Moreover, sharing coordination position, the characteristics of each component, such as the radii or electronic density, are a combination that make unique each structure, and distinguish the correct catalyst for different reactions. Therefore, it is modelling nature of cations (bi- and tri- valent) and of anions, that is possible change the behaviour in the reactant system.

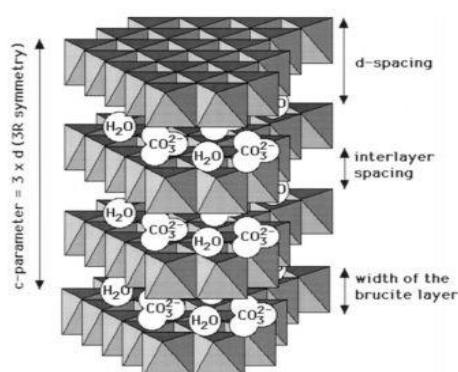


Figure 3: Hydroxalite intra-layer structure (Cavani, et al., 1991).

In the present work, Mg is used as bivalent metal, M(II); Al as the trivalent one, M(III) and CO₃²⁻ as anion; the cumulative charge on the material surface is a balance between both two contributes. The chosen x value is 0,30 (2:1=Mg:Al), even if can vary from 4:1 and 2:1 ($0,20 \leq x \leq 0,30$), additionally, also x value affects strongly material's properties. However, although each component influences acid-base state, many studies reported also trend of HTlcs to incorporate CO₂ from the air; even if the anion is itself the carbonate. In this case the acid properties of the material play major role. At the same time after thermal treatment, interlayer anions are lost and releasing on the surface OH⁻ species, Brønsted base sites. On industrial scale, there are several base catalysts, depending from the specific use, briefly:

- Alkylation: usually, alkylation of phenol with methanol or o-xylene with butadiene, are carried out with MgO₂ and K₂CO₃/Na (promoter);
- Isomerization: 1,2-propadiene is isomerized using K₂O/Al₂O₃;
- Dehydration/condensation: as catalyst can be used oxides Zr based (ZrO₂) for dehydration of 1-hexylethanol and for the one of iso-butyraldehyde;

- Esterification: for example, the one of ethylene oxide with alcohol is carried out with hydrotalcite (Cavani, et al., 2009).

During this process, the material is activated and can be used as a solid base catalyst. The thermal decomposition sequence of Mg-Al-CO₃ HTlc has been well reported (Hibino, et al., 1995): Mg-Al-CO₃ HTlcs converts to Mg-Al double oxide at 400°C, increasing the temperature, with the movement of the Al ions, there forms a double oxide phase that decomposes at 900°C in a spinel phase (MgAl₂O₄) and MgO. When the temperature is between 400°C and 800°C the HTlc structure can be obtained from the spinel phase structure, using an aqueous solution. In this work has been reported the try to carry out the reconstruction under wet nitrogen flow, studied for different treatment time. After this paper the same authors (Kosuge, et al., 1996), noted that some Mg-Al-CO₃ HTlcs reconstructed yielded spinel phase and MgO at 400°C. Mg-Al spinel can be considered prominent materials due to their good properties as high melting point, high hardness, high chemical stability and good optical transmission. These make the material a good choice not only as a catalyst support (Shen, et al., 1994), but also as a catalyst itself. As shown different authors, the surface basic properties, and consequently catalytic performance, depend on the acid-base pairs Me⁺ⁿ and O²⁻ and O²⁻ anions. The basic properties of magnesia are modified and controlled through the replacement of Mg²⁺ with guest ions in the lattice, indeed Al³⁺ (Bolognini, et al., 2003). These ions develop a coordination vacant in the structures, which attracts part of the electron density on oxygen. Depending on these and on the Mg/Al ratio, that modifies the amount of vacant sites on the structure, the surface has a different number of sites: on one hand, sites with strong basicity (O²⁻ anions), which are deeply prone to interact with the molecules of the substrate. On the other hand, sites with a weaker basicity (Me⁺ⁿ and O²⁻), which react less with the reaction environment. This duplicity have efficient application in catalysis, leading the hydrotalcite materials as a potential substitutes for the most common bases used in industry (Bastiani, et al., 2004); moreover it is possible create a poly-functionalised catalyst, and combine more reactions on its surface.

1.6.2 Synthesis of a hydrotalcitic material

HT are conventionally synthesised by co-precipitation method (CP), anyway the synthesis can be carried out by sol-gel method (SG) (Miller & Ko, 1997); the SG pathway is used when a good component mixing is reached, this means that is possible

control the homogeneity of the species in the structure, thereby the material properties such as acid-base properties. However, the good mixing may not be the goal reached and the CP method can be chosen while easily handling and less costly, using in fact, metallic alkoxides and preformed sols.

The CP method involves oxide precipitation of the precursor, dropping alkali hydroxide and carbonate as pH regulators (Shen, et al., 1994) (Cavani, et al., 1991). As well reported, following the CP procedure, residues of K and Na leach on the surface of the catalyst (D.G. Cantrell, 2005); their real presence, during heterogeneous catalysis, may contaminate the resulting product, making difficult also the performance comparisons of the catalytic efficiency with different materials.

1.6.3 Synthesis of a hydrotalcitic material via alkali-free method

As reported above, using an alkali-free method during the precipitation, may be better in order to have a cleaner product. A possible route is synthesise Mg-Al hydrotalcite using a different precipitant agent, having cleaner conditions; one example can be $(\text{NH}_4)_2\text{CO}_3$ and NH_4OH . Even if they are weaker base component, and easily NH_3 is produced and easily escape, the precipitation occurs with a slower reaction time. Moreover, a slower precipitation may have a positive consequence: expanding the process time, each component has enough time to an ordered coordination. However, if K and Na affect the structure of the catalyst, can enter in the reaction mechanism as a physical promoter, increasing the surface area, at the same time both may take part of the reaction. Fortunately, as reported (Woodford, et al., 2012), displacing the alkali with the free-one, this change has no effects on the Mg-Al ratio. Nevertheless, that both conventional methods and the alkali-free methods offer limited control on the morphology, particles size, surface area and pore architectures; all these properties are important when the catalytic performance are reached. Macroporous materials, with a designed structure, can have several applications in the catalysis field; the porosity, in fact, may act as a molecular sieving, which is able to release or hold some products instead others. Thus it is tried to study how the different size of catalyst's pores may affect the reaction yield; reaching these goals, two methods have been develop to have a higher range of usable pores sizes.

1.6.4 Templating Agent

As said, the using of catalyst with an ordered structure for transesterification reaction may have several advantages; pores on solid surface with different size, can have a specific behaviour depending for example by reactants dimension, and in our case, by the length of triglyceride's chains.

The attachment of organic functionalities to the surface of the silica mesoporous supports has been an interesting research area in heterogeneous catalysis and green chemistry during the last years. Because of their ordered and uniform porosity, this kind of material is very interesting for applications such as catalysis, adsorption, chromatography or host-guest-chemistry.

View papers reported, in their work efficient methods to prepare ordered macroporous layered double hydroxides, by coprecipitation of divalent and trivalent metal cations in the interstices of a colloidal matrix containing a sprinkled material, such as polymer spheres (E. Géraud, 2006). These spheres, so called templating agent, can be removed by dissolution or during the thermal treatment of the Mg_2Al HTlc after infiltration-precipitation and drying process. Studies show also the capacity of the metal oxides materials to reconstruction either by exposure at high relative humidity or after immersion in water. Hypothetically, there are no high limitations on the nature of the templating agent, but for the decomposition temperature; different studies reported the use of templating agent as polystyrene (PS) spheres.

Here the meaning of Hydrotalcite-like compounds grow up, referring to materials like Hydrotalcites, about the nature of components, whereas the meaning of "like compound" is due to the templating agent's role to design a specific structure.

In the present work will be tested either PS or poly(methyl methacrylate) (PMMA) spheres of different sizes. The poly(methyl methacrylate) nanoparticles synthesis is reported by Norakankorn et al., for which the sizes range is from 50nm to 120nm, with large possible choices. One of our aims was explore the range of the possible PMMA spheres' diameter; with this aim two parameters have been studied: the volume of water where conduct the reaction and the amount (g) of surfactant to use (SDS).

2. EXPERIMENTAL

The present work has been developed on different areas of interest: synthesis of catalysts with different physical and structural properties, such as porosity and surface area, thermal behaviour; synthesis of polymeric materials to use as structural templating for the catalyst and catalytic tests on transesterification reaction using triglyceride, with different chain length, and methanol.

2.1. Catalyst synthesis

2.1.1 Conventional Hydrotalcite

The first tests were carried out in order to obtain conventional hydrotalcite like compounds (HTlc) based of atomic ratio Mg/Al as 2, according with the procedure alkali-free reported (D.G. Cantrell, 2005). In a round bottom flask reactor 50 cm³ of de-ionized water was heated up to 60°C under vigorous stirring; reached the conditions, 100 cm³ of an aqueous solution 0,2 mol of (NH₄)₂CO₃ was added to the reactor. 100 cm³ of an aqueous solution containing the precursors Mg and Al, respectively 0,1 mol and 0,5 mol, was dropped slowly to the starting solution over about 1,5 h. The pH was left decrease spontaneously to 7,8-8 and then kept constant by drop wise addition of 35% aqueous ammonia solution. After the addition, the material was aged for 3h at the same pH and temperature under vigorous stirring; the precipitate was filtrated under vacuum technique and washed with water (2L) obtaining a neutral pH. The solid was dried overnight at 80°C otherwise at 110°C for 4h. The obtained conventional HT (ConvHT) were processed with thermal treatment, first under O₂ flow (20mL/min) and then under wet N₂ flow (100mL) to obtain the reconstructed material.

2.1.2 Macro-porous Hydrotalcite (PS)

In order to have a material structurally ordered, it was decided to conduct the material's synthesis in presence of a so-called, templating agent, a polymer in the form of spheres with different size. With this aim, polystyrene spheres, with a diameter of 280nm and of 750 nm, were added during the synthesis of the HTlc following the procedure reported (Woodford, et al., 2012). Briefly, in a round bottom flask reactor, were added 6g of PS beads and 25 cm³ of a solution 1:1 of de-ionized water and ethanol, the mixture was heated at 60 °C and kept under vigorous stirring. Reached the conditions, 100 cm³ of an

aqueous solution 0,2 mol of $(\text{NH}_4)_2\text{CO}_3$ was added to the reactor. 100 cm³ of an aqueous solution 1:1 of water and ethanol, containing the precursors Mg and Al, respectively 0,1 mol and 0,5 mol, was dropped slowly to the flask over about 1h. The pH was left decrease spontaneously to 7,8-8 and then kept constant by drop wise addition of 35% aqueous ammonia solution. After the addition, the material was aged for 3h at the same pH and temperature under vigorous stirring; the precipitate was filtrated under vacuum technique and washed with water (2L) obtaining a neutral pH. The solid was dried overnight at 80°C. The obtained macro-porous HT (HT-PS) were processed with thermal treatment, first under O₂ flow (20mL/min) and then under wet N₂ flow (100mL) to obtain the reconstructed material. For HT-PS the calcinations process is used, not only to eliminate the carbonate from the structure and activate the materials by transition phase, but also to burn the templating agent. Due that, after the complete oxidation of the polymer to CO₂ and the thermal degradation, the purpose was obtain a regular structure by the shape of the PS spheres.

2.1.3 Meso-porous Hydrotalcite (PMMA)

In order to investigate the consequences of a different porosity on the catalyst surface for the reaction, was been used colloidal dispersion of poly(methyl methacrylate) spheres in an aqueous matrix. Briefly, in a round bottom flask, were added 6g of solution where PMMA beads were been synthesized and 25 cm³ of a solution 1:1 of de-ionized water and ethanol, the mixture was heated at 60 °C and kept under vigorous stirring. Reached the conditions, 100 cm³ of an aqueous solution 0,2 mol of $(\text{NH}_4)_2\text{CO}_3$ was added to the reactor. 100 cm³ of an aqueous solution 1:1 of water and ethanol, containing the precursors Mg and Al, respectively 0,1 mol and 0,5 mol, was dropped slowly to the flask over about 1,5 h. The pH was left decrease spontaneously to 7,8-8 and then kept constant by drop wise addition of 35% aqueous ammonia solution. After the addition, the material was aged for 3h at the same pH and temperature under vigorous stirring; the precipitate was filtrated under vacuum technique and washed with water (2L) obtaining a neutral pH. The solid was dried overnight at 80°C. The obtained macro-porous HT (HT-PMMA), were processed with thermal treatment, first under O₂ flow (20mL/min) and then under wet N₂ flow (100mL) to obtain the reconstructed material. As for the HT-PS, also for the HT-PMMA, the thermal process was due to burn the templating agent, reaching the porosity, to eliminate the interlayer anions carrying the transition phase.

2.2 Material Characterisation

The different catalysts have been characterized by different techniques: XRD porosimetry analysis, TGA, SEM-EDX, TEM-EDX, MP-AES, and, CO₂ titration before and after the calcinations process.

Thermal treatments under wet nitrogen flow were carried out with different during time, in order to investigate the ability of the materials reconstruction. Tests were carried for 24 h and 48 h starting at 250°C up to 450°C and cooling spontaneously at room temperature. The re-enactment ability was tested by XRD analysis, comparing the patterns obtained from the materials in each steps. Powder XRD patterns were recorded on a PANalytical X'PertPro diffractometer fitted with an X'celerator detector and Cu-K α source for $2\theta = 5-80^\circ$ with a step size of $0,02^\circ$. The raw data were studied with Xpert-data analyzer software. The Scherrer equation was used to calculate HT crystallite sizes. Porosimetry analyses were carried out in order to study the surface area, pore's size and volume pore distribution Nitrogen porosimetry was undertaken on Quantachrome Nova 1200 and Autosorb Porosimeters. Samples were degassed at 120°C for 2h prior to analysis. Multi-point BET surface areas were calculates over the relative pressure range 0,01-0,3. Pore volumes were calculating applying BJH methods to the desorption isotherm for relative pressure $<0,02$ and $>0,35$. In order to investigate the thermal behaviour of the materials thermogravimetric analyses were performed using a StantonRedCroft STA780 Thermal Analyser, under Oxigen and Nitrogen follow 20 ml/min, heating 10°C/min up to 800°C.

SEM analyses were carried out on Oxford Instrument EVO SEM, placing the samples onto a carbon disc on an aluminium stub. Energy dispersive X-Ray (EDX) analysis was also carried out using the Oxford Instruments Inca Software. Base site densities were measured *via* CO₂ pulse chemisorptions titration on a Quantachrome ChemBET 3000 system. Semples were outgassed at 120°C under flowing He (120ml min⁻¹) for 1h, prior to CO₂ titration at 40°C. High-resolution TEM was carried out on a Philips EM208 TEM operating at 80kV with a Tungsten filament. Energy dispersive X-Ray (EDX) analysis was also carried out using the Philips EM208 TEM. Samples were deposited from ethanolic solution onto holeycarbon copper grids.

2.3 Poly(methyl methacrylate)

2.3.1 Poly(methyl methacrylate) synthesis

PMMA nanoparticles are prepared by micro-emulsion polymerization following the method reported (Norakankorn, et al., 2007). In a 500 cm³ Pirex glass reactor, was added de-ionized water (in the range of 60-100 cm³); stirring at 200 rpm and feeding with nitrogen flow for 30 min. Surfactant, sodium dodecyl sulphate (SDS), and initiator, azo-isobutyronitrile (AIBN), were added to the reactor; keeping inert and dark conditions: cover the reactor with aluminium to avoid the interaction of the initiator with the light. The mixture was heated at 60 °C and kept under vigorous stirring; equipping the reactor with a condenser and a dropping funnel. Reach the condition, monomer is added slowly (around 1,5h) through the dropping funnel, (a drop each 8 sec). At the end of addition, the system was kept at 70°C under vigorous stirring for 1h (to obtain a higher yield of the polymer).

2.3.2 Separation of the polymer for Characterization

The polymer is precipitated using methanol as anti-solvent (150mL) and washed using three times a solution of warm water and methanol (1:1) dividing the solid from the liquid through a centrifugation (9000 rpm for 15 min).

The final extraction is made with cyclohexane in order to removed the monomer not reacted, with this aim, the solid is put in a round bottom flask adding cyclohexane. The system is stirred (500rpm) and heated at 40°C for 24 h equipping the round bottom flask with a closed condenser; at the end of the extraction, the solid is recovered by vacuum filtration. The sample is dried in the oven at 40°C for 2h.

2.3.3 Characterisation of the PMMA nano-spheres

After the polymerization was completed, the number-average diameter (D_n) of the particles was measured using a dynamic light scattering technique with a DLS, Brookhaven Instrument Corp. and reported on a ZetaPlus Particle Sizing Software. SEM analyses were carried out on a Oxford Instrument EVO SEM, placing the samples onto a carbon disc on an aluminium stub. In order to investigate the thermal behaviour of the materials thermogravimetric analyses were carried out with StantonRedCroft STA780 Thermal Analyser; under Oxygen and Nitrogen flow 20 ml/min, heating 10°C/min up to 800°C.

2.4 Transesterification reaction

The transesterification tests were carried out on a Carousel 12 Plus Radleys with heating and magnetic stirring. A glass tube was charged with 50 mg of catalyst, 10 mmol of individual saturated triacyl glycerides $C_3H_5(OOR)_3$ with $R = C_4$ and C_8 , and 30 mmol of methanol using, as internal standard, dihexyl ether (0,0025 mol) and heated up to $60^\circ C$. In order to better solubilise the triglyceride C_8 , it was added butanol. The same procedure was followed for the triglyceride C_4 in order to investigate the influence of butanol during the reaction. Aliquots were periodically withdrawn and filtered prior to detailed analysis of TAG conversion and FAME production on a Varian450GC, with 8400 autosampler.

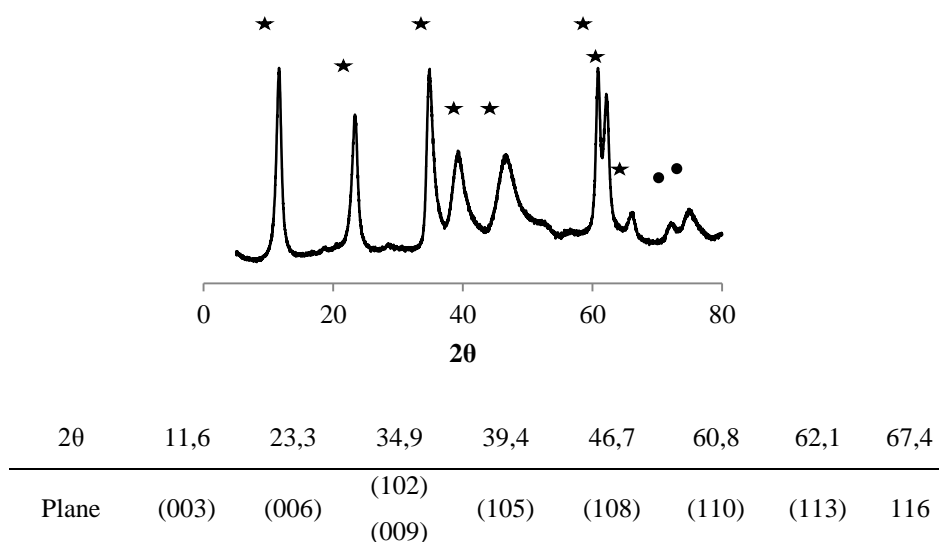
3. RESULTS

During this section of the present work, the Conv HT and HT-PS will be considered separately from the HT-PMMA materials.

3.1 Catalyst Morphology

3.1.1 XRD

The obtained HT materials, conventional type and macro-porous, have been calcined, first under O₂ flow (20mL/min) and after under wet N₂ flow (100mL) for 24 h and 48 h to test the so called “memory effect” and the reconstructs efficiency by hydration. For macro-porous HT-PS the calcinations process is used, both to eliminate the carbonate from the structure, activating the materials by transition phase, and to burn the templating agent. Actually, after the complete oxidation of the polymer to CO₂ and the thermal degradation, the purpose is obtain a regular structure by the shape of the polymeric spheres. The calcinations process leads a phase changing of the HTlc, from Mg and Al hydroxides to mixed oxides, from which, the original phases may be rebuilt after an hydro treatment. Usually, the re-enactment is possible adding the calcined HTlc to boiling water; in order to simplify the process, it was chosen to carry the rebuilt under wet nitrogen flow.



Graph 1: X-Rays diffraction pattern: (★) CONV-HT Mg-Al-CO₃ at room temperature; (●) reflections due to impurity Al₂O₃

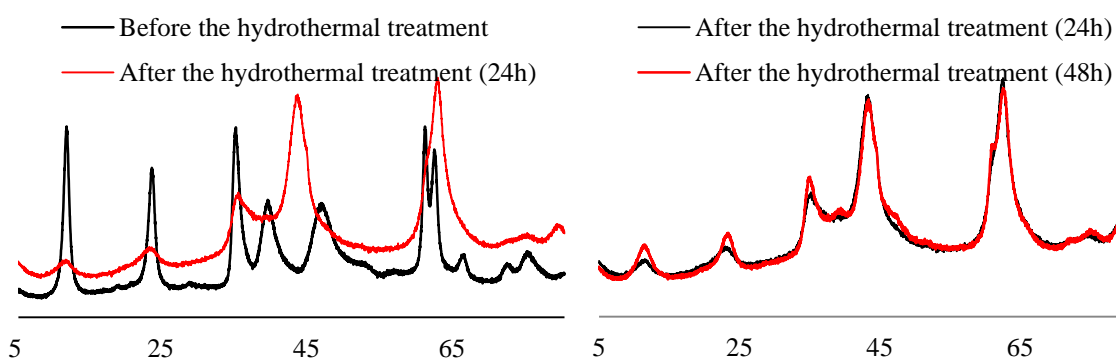
By XRD analysis, was tested the re-enactment ability, comparing the patterns obtained from the materials in each steps. The typical HTlc's pattern was recorded on the CONV-HT before the calcinations process in order to identify the most intense diffraction peaks (**Fig. 1**). The (00*l*) reflections are characterised by high intensities combined with a broad lineshapes indicating that the hydrotalcite has an high level of crystallinity and very small crystallite. The crystallites sizes were calculated from the (003) and (006) using the Debeye-Scherrer equation:

$$\tau = \frac{0,89\lambda}{(\beta(\theta)\cos\theta)}$$

Where τ is the crystallite size; λ is the wavelength used during the analysis; $\beta(\theta)$ is the full width at half maximum (FWHM) and θ is the Bragg diffraction angle.

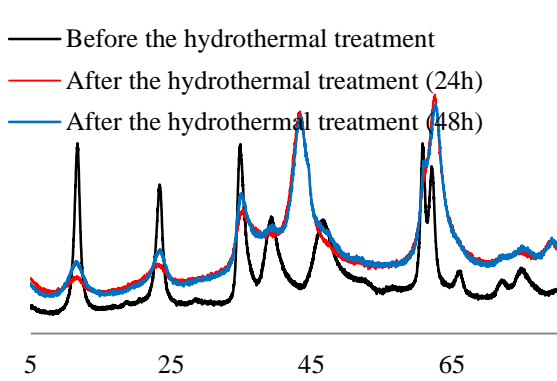
Thank HT patterns after calcinations, it has been possible identify the characteristic peaks of mixed oxides phase and with that compare the x-rays diffraction patterns obtained with the HT-PS280 and HT-PS750 during the different steps(**Graph2-13**).

The process of hydration due to wet N₂ flow, does not seem be sufficiently effective when it takes 24 hours; the observed trends are comparable to those compounds subjected only to calcinations process, typical of mixed oxides. When the hydro treatment takes 48 hours, it is observed a partial tendency of the material to rebuild, even if the rebuilt of the hydrotalcite structure is not possible at all. The HT-PS materials show some predisposition to be re-enacted, anyway their “memory effect” seems lower than the one shown by the CONV-HT. It may suppose that being pores that bring to a decrease of surface area (see the porosimetry analyses), the interaction of water with the material is lower.

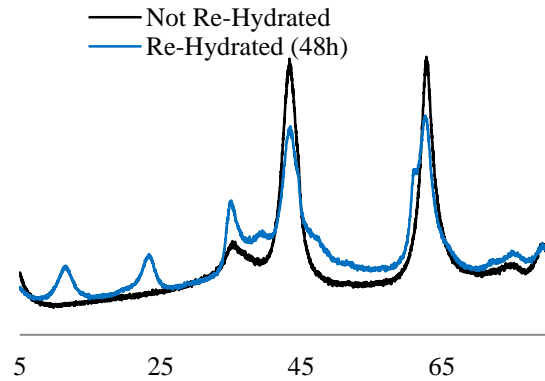


Graph 2: XRD Pattern of the ConvHT before and after the calcinations process.

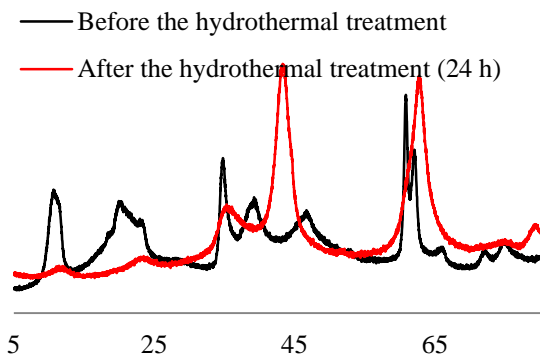
Graph 3: XRD Pattern of the Conventional HT after thermal treatment and wet N₂ flow for different hydration time.



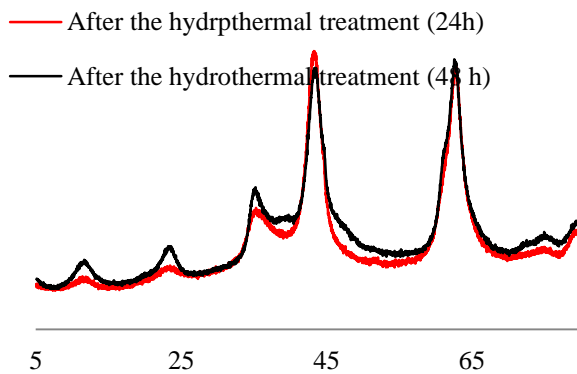
Graph 4: Comparison between each ConvHTlc after every step.



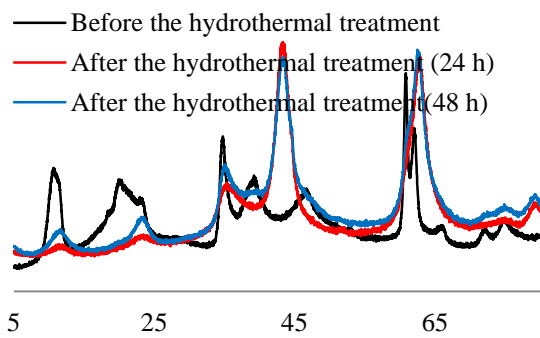
Graph 5: Comparison between hydrated ConvHTlc and mixed oxides Mg-Al-O.



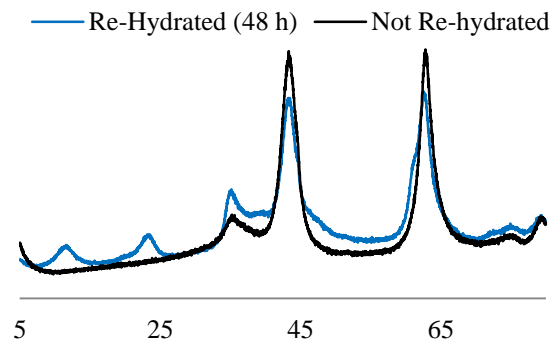
Graph 6: XRD Pattern of HT-PS280 before and after the calcinations process.



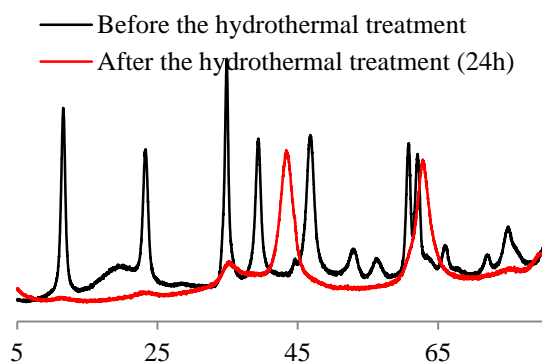
Graph 7: XRD Pattern of HT-PS280 after thermal treatment and wet N2 flow for different hydration time.



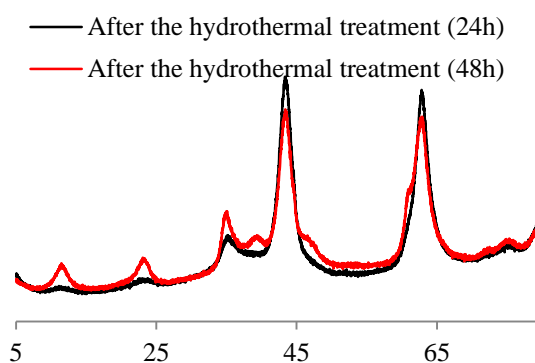
Graph 8: XRDs Comparison between each HT-PS280 after every step.



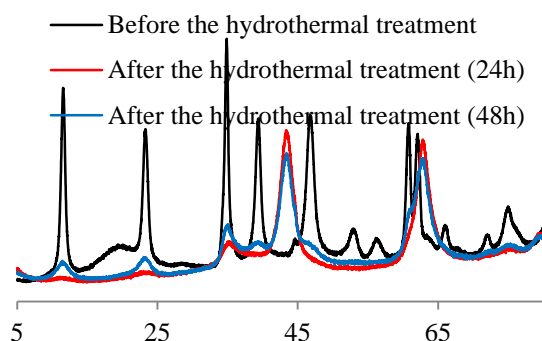
Graph 9: XRDs Comparison between hydrated HT-PS280 and mixed oxides Mg-Al-O.



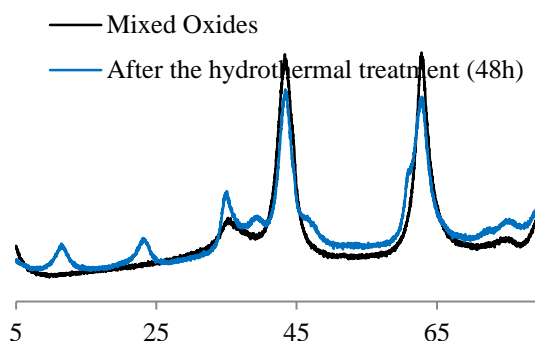
Graph 10: XRD Pattern of HT-PS750 before and after the calcinations process.



Graph 11: XRD Pattern of HT-PS750 after thermal treatment and wet N₂ flow for different hydration time.



Graph 12: XRDs Comparison between each HT-PS750 after every step.



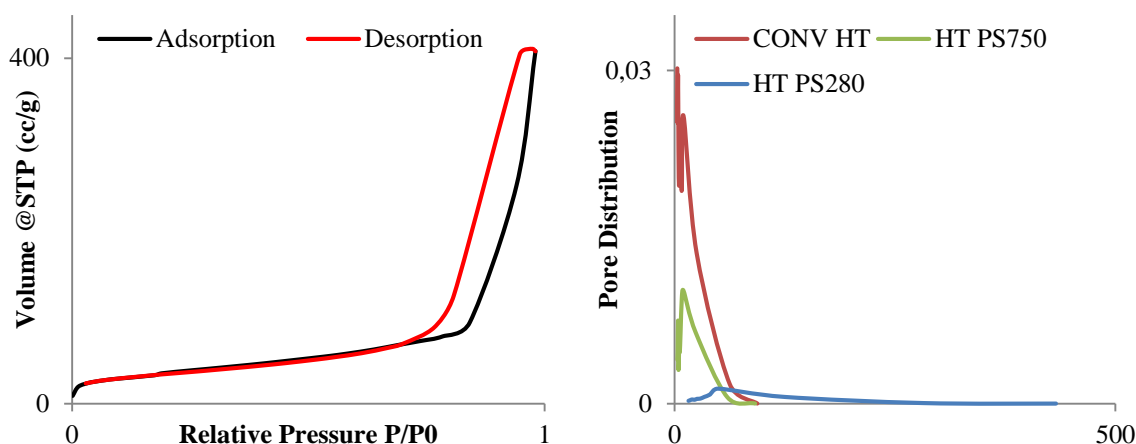
Graph 13: XRDs Comparison between hydrated HT-PS750 and mixed oxides Mg-Al-O.

3.1.2 Porosimetry analyses

Porosimetry analyses were carried out in order to study the surface area, pore's size and volume of the HTlc and their possible differences about the N₂ adsorption and desorption. As expected, the hydrothermal treatment duration time does not lead to differences at surface area values; the trend, in both cases, shows hysteresis behaviour (**Graph 14**). The hysteresis behaviour is due to the porosity and tortuosity of materials, from which the relative pressure is less during desorption than the adsorption. The BET model describes this kind of behaviour with the Isotherm BET Type IV, and by which is related to a multilayered adsorption of N₂. The surface area data are showed on **Table 6**, from the results is possible notice that the HT have a surface area bigger than the HT-PS. The two macro-porous materials, HT-PS280 and HT-PS750, seem have the same surface area even using a different size of templating agent.

	HT	HT-PS280	HT-PS750
Surface Area (m ² /g)	233	80	70
Pore Diameter (nm)	3,1	3,9	10,1
Pore Volume (cc/g)	0,65	0,66	0,25

Table 6: Porosimetry results for ConvHT, HT-PS280 and HT-PS750.



Graph 14: N₂ adsorption and desorption on catalyst surface and pore size distribution of hydrotalcite materials as function of the templating agent.

3.1.3 SEM

SEM analyses were carried out on the conventional HT to confirm the well turned out of the synthesis, and on the meacroporous HTlc to confirm the real structural order of materials. The results, obtained for the conventional type, are then shown on **Image 1**. The SEM picture show the well-known "sand roses" structure of hydrotalcitic materials verifying consequently the right reaction conditions used, such as pH, temperature, concentration of reactants etc. SEM analyses were also conducted on HT-PS280 (**Image 2-3-4**), and show the partial regular structure of the material conferred by the polystyrene spheres. During the analysis, it was possible to measure the diameter of the pores ensuring the right work of the templating agent. As shown in **Image 3**, the templating agent print (291.5 nm) has a size complying with the PS particles' diameter (280±30 nm). Hypothetically, it may be allowed increase the pores distribution, increasing the amount of PS beads. SEM analyses were also carried on HT-PS750 (**Image 5**); the pictures show how the templating has not been properly incorporated into the structure, for that is possible see the typical structure of a conventional HTlc, with sand roses' shape. HT-PS750 lacks of an ordered structure given by templating agent; it can be

supposed that the PS beads, during the calcinations process, have been burned without leaving their print and after thermal decomposition the entire structure has been destroyed. Moreover, the diameters of the beads could be too high for the low amount of the synthesised HTlc; for that, during the calcinations, the HTlcs suffered a decreasing of surface area, as shown by BET analysis.

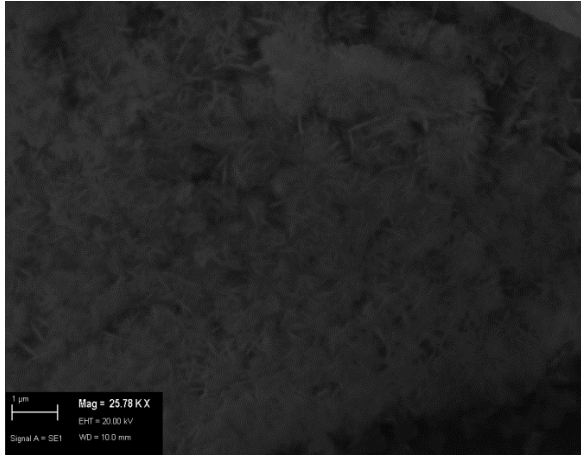


Image 1: Conventional HT by SEM analyses with the sand's roses.

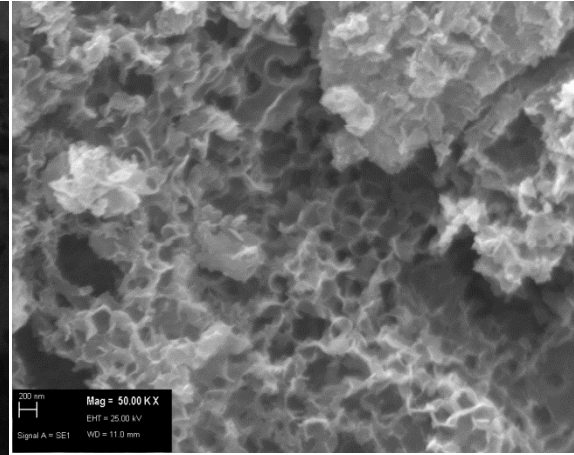


Image 2: HT-PS280 by SEM analyses.

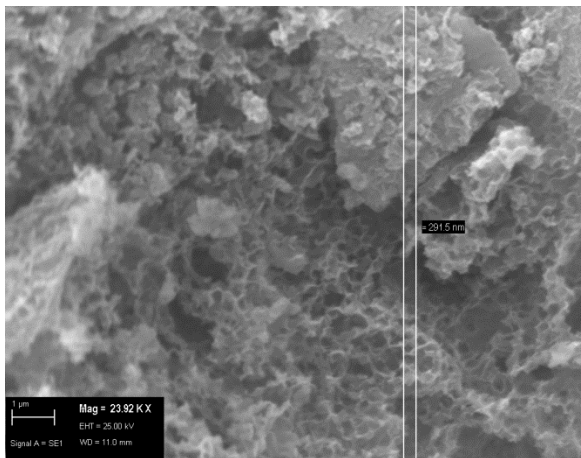


Image 3: HT-PS280's pore size by SEM analyses.

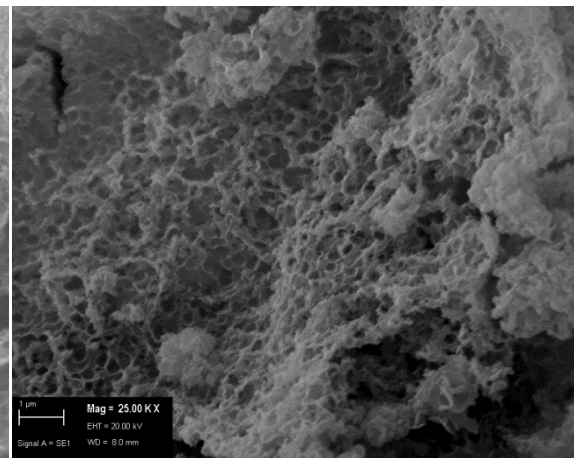


Image 4: HT-PS280 by SEM analyses.

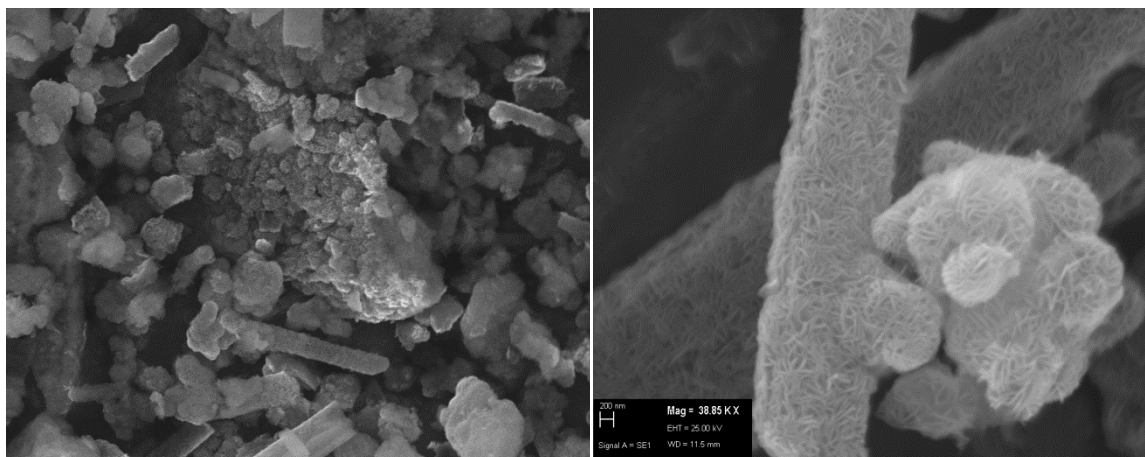


Image 5: HT-PS2750 by SEM analyses with a different magnification.

3.2 Catalyst Composition

3.2.1 MP-AES, EDX and TGA

The real Mg/Al of the ConvHT and HT-PS280 was undertaken by MP-AES and EDX analyzes; the results obtained are shown in **Tables 7-8-9-10**, and these show the right carried out of the reaction.

	λ (nm)			
Atomic Amount	279,553	280,271	383,829	Average
Mg	50,68	50,82	52,49	51,33
	λ (nm)			
Atomic Amount	308,215	394,829	396,152	Average
Al	26,71	27,87	28,32	27,63
Ratio Mg:Al				1,86

Table 7: MP-AES analysis for Conventional Hydrotalcite, CONV-HT.

	Test 1	Test 2	Test 3	A.A.(%) Average
C	14.09	14.57	22.65	Mg:
Mg	18.27	17.41	10.61	15.43
Al	8.47	8.59	4.33	Al:
O	59.16	59.43	62.41	7.13
Ratio Mg:Al				2.16

Table 8: EDX analysis for Conventional Hydrotalcite, CONV-HT.

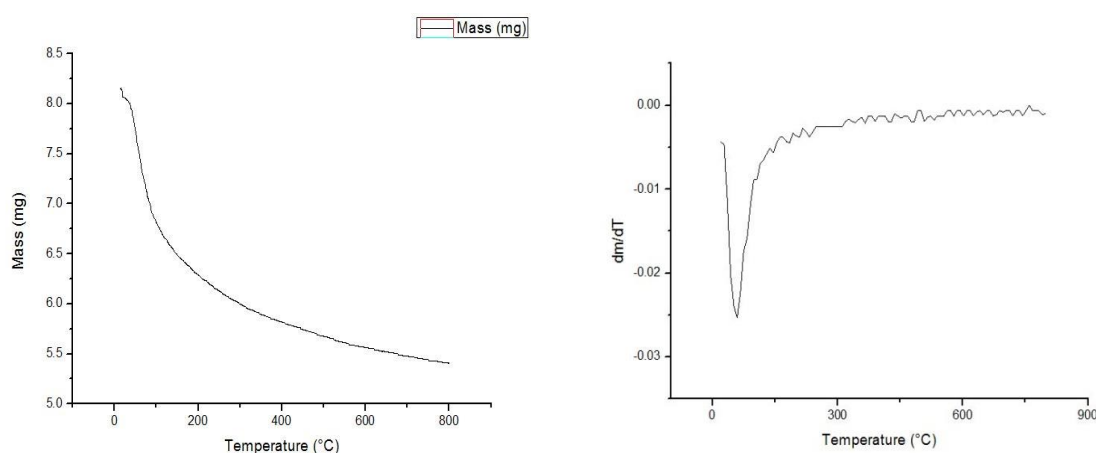
	Test 1	Test 2	Test 3	Test 4	A.A. (%) Average
C	28.44	24.41	14.70	4.49	Mg:
Mg	5.23	9.18	17.94	25.94	14.57
Al	1.69	3.37	8.01	13.97	Al:
O	64.64	63.05	59.35	55.71	6.73
Ratio Mg:Al					2.16

Table 9: EDX analysis for Meso-porous Hydrotalcite, HT-PS280.

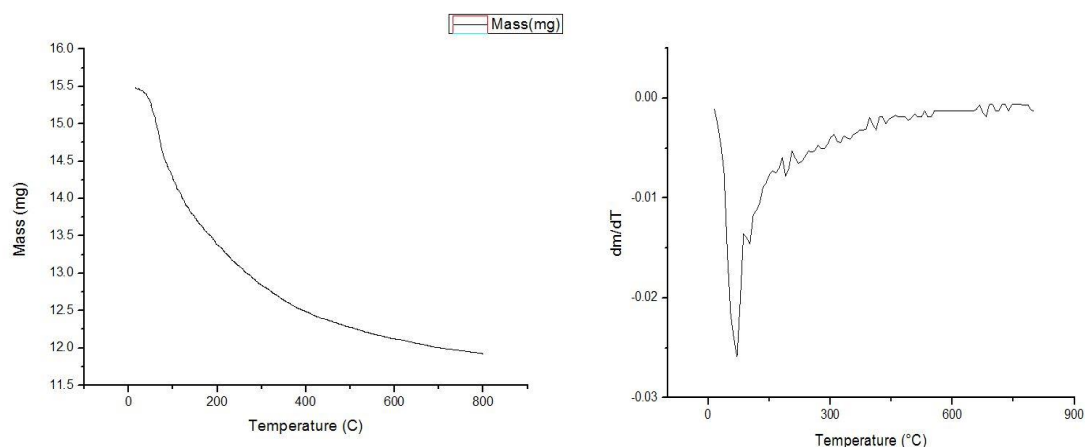
	Test 1	Test 2	Test 3	A.A. (%) Average
C	18.21	15.82	14.18	Mg:
Mg	13.35	16.74	19.38	16.49
Al	5.89	7.57	8.42	Al:
O	62.55	59.88	58.02	7.29
Ratio Mg:Al				2.26

Table 10: EDX analysis for Meso-porous Hydrotalcite, HT-PS750.

In order to investigate the thermal behaviour of the material, CONV-HT and HT-PS280, after the calcinations and re-hydration processes, thermogravimetric analyses were carried out (**Graphs 15-16**). The graphs show the same trends for both conventional type's material and structural ordered material, which it is possible to observe the water loss close to 100 °C, anyway the amount of water loss, between the two materials, is different for a 10% (**Table 11**).



Graph 15: Conventional HT after Hydrothermal process and differential behavior dm/dT v.s. Temperature.



Graph 16: HT-PS280 after Hydrothermal process and differential behavior dm/dT v.s. Temperature.

	Conv-HT	HT-PS280
Water loss (%)	33,6%	23,1%

Table 11: Mass loss (%) of CONV-HT and HT-PS280 in TGA analyses.

According with XRD analyses and porosimetry analyses, the attitude of conventional HT to incorporate water, is higher than the HT-PS280. Consequently, it is observed a higher water mass loss.

3.3 PMMA Characterisation

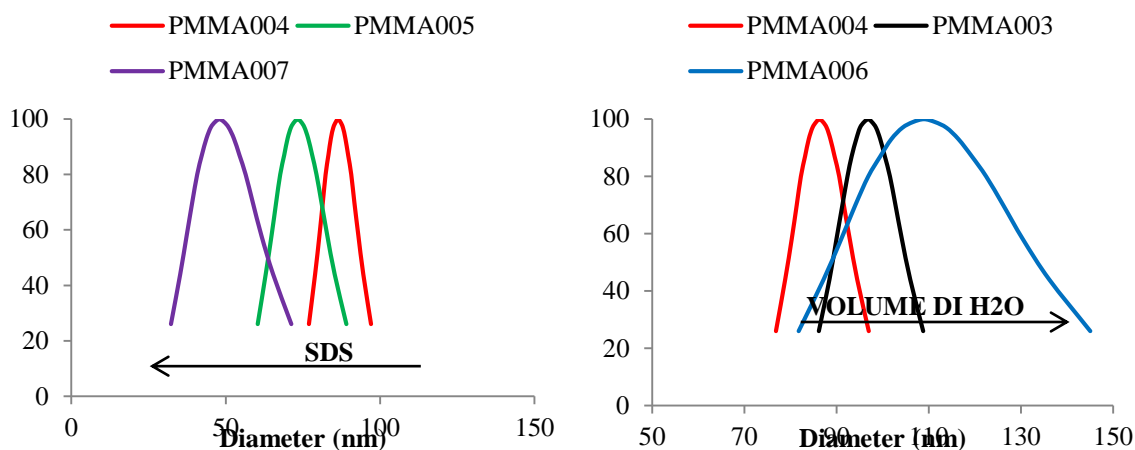
3.3.1 DLS

The aim was use a new templating agent during the HTlc synthesis, in order to change the pores size. Several tests were conducted in order to explore the range of the possible PMMA spheres' diameter; with this aim, two parameters have been studied: the volume of water where conduct the reaction and the amount (g) of surfactant to use (SDS).

Test	Diameter (nm)	SDS (g)	H2O (ml)
PMMA006	127,7±1,1	0,098	98
PMMA003	99,1±0,5	0,098	84
PMMA004	88,4±0,5	0,098	60
PMMA005	79,3±0,5	0,016	60
PMMA007	66,5±0,5	0,31	60

Table 12: Particle Sizes obtained during the PMMA syntheses with different reaction conditions.

The amount of monomer (MMA) and initiator (AIBN) were kept constant, with different ratio. By the trends (**Table 12** and **Graph 17**), it is possible conclude that smaller size of PMMA nanoparticles are reached, increasing or the SDS amount (grams), with the same volume of water, AIBN and MMA; or decreasing the volume of water (ml), keeping SDS, AIBN and MMA constants.



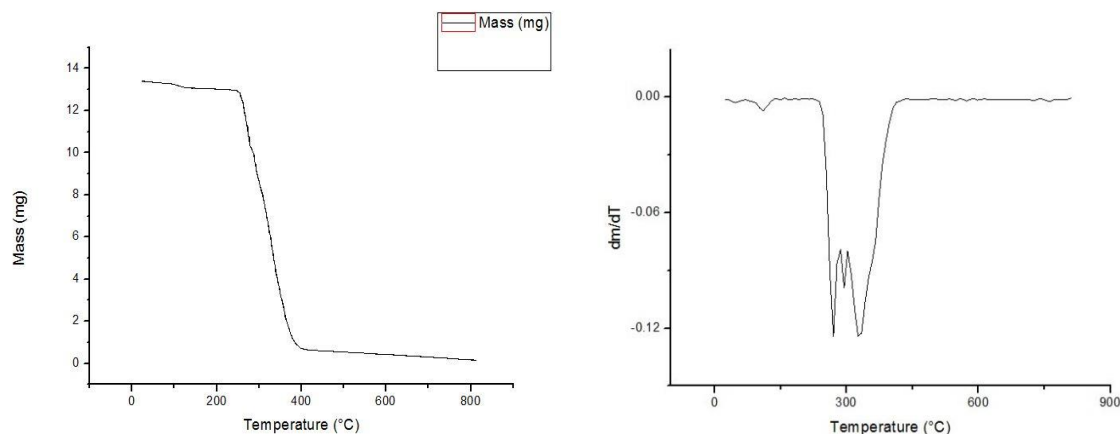
Graph 17: PMMA sizes trends changing first SDS amount (graph left), and then the water volume (graph right)

The graphs show a loss of reaction efficiency when that is carried out in larger volumes of H₂O leading to a wide distribution of diameters of the nanoparticles, that is shown by the bigger shape of the curves which the SDS grams and H₂O volume are higher. The PMMA006 curve, blue coloured appears quite enlarged compared to the other, more narrow and peaked; the same behaviour it's showed by the PMMA007 curve, purple. When or the volume of water or the SDS amount increase too much, the size's control is significantly reduced, or lost. The particles diameters have been studied by DLS; in **Table 12** are shown the results and the amounts used each test.

3.3.2 TGA and SEM

The PMMA solution, obtained after the aging time, is colloidal type, in which the polymer's particles are dispersed in the liquid phase; broken the heterogeneous mold seemed hard to have. Reaching the characterisation purpose, have been used different techniques, such as centrifugal separation technique and vacuum filtration with Buchner funnel in order to divide the liquid from the particles, or vacuum oven and rota-vapour to evaporate the liquid leading the solid. Working with techniques which use heat and vacuum condition, is possible the denaturation of the polymer, nevertheless that the

polymer has its degradation and decomposition temperatures, around 70 °C, and the environment is aqueous. The amount of solid PMMA, recovered by centrifugal technique, was studied by thermogravimetric analysis (TGA/DTA) to check the purity of the sample recovered. The results are shown on **Graph 18**.



Graph 18: PMMA under thermal treatment and differential material's behaviour; dm/dT v.s. Temperature.

From the decomposition behaviour, the material loses 100% of its mass once are reached 400°C; the four different mass variations are in a temperature range of fairly limited and are attributable to different states of polymer decomposition:

- I degradation step initiated by radical transfer due to the unsaturated chain;
- II and III homolytic radical degradation step of the chain and degradation initiated by radical transfer to unsaturated ends;
- IV peak random scission.

The decomposition behaviour obtained, is similar to those present in PMMA literature.

To verify shape and size of the particles SEM analyses were carry out. The SEM picture (**Fig. 27**) shows the PMMA nano-spheres, recovered by simple centrifuge and dried by the remaining liquid at room temperature; the other one (**Fig. 28**) shows PMMA, in the solid state, obtained by vacuum oven drying at 35 °C.

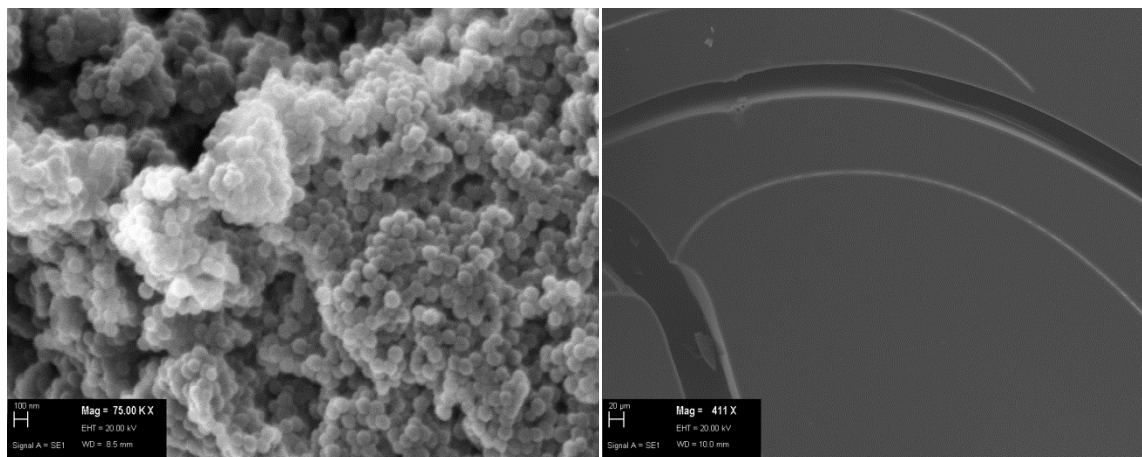


Image 6: PMMA's particles dried at room temperature and recovered by centrifugal technique(left)- PMMA amorphous phase obtained by vacuum technique(right).

It is possible observe how the vacuum treatment has led to glass transition point of the material, causing its denaturation; at the same time leaving the sample to the air, when the solvent evaporation is spontaneous, the beads seem maintain their nature (**Fig. 27**).

3.4 HT-PMMA Characterisation

The considerable problems to obtain a large amount of polymer by centrifuge and filtration, in order to overcome the nanoparticles dispersion breakage, it was decided to precipitate the cationic precursors, Mg and Al, used in the synthesis of HTlcs, in the aqueous colloidal solution where PMMA particles are contained. The used conditions are the same to those used during the HT-PS synthesis, adding 6 g of the solution containing the PMMA nano-spheres. The purpose of this method was to carry out the HTlc synthesis where the templating agent was already distributed in the reaction environment. With this aim, different HT-PMMA materials were synthesized using different colloidal solution containing PMMA spheres.

3.4 XRD and EDX

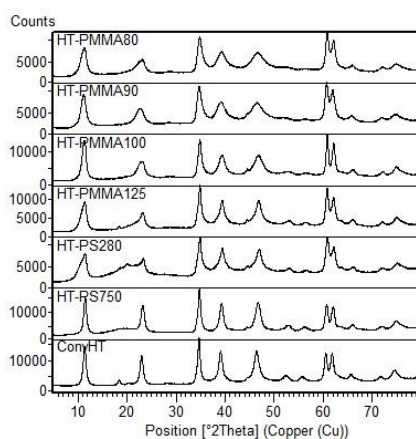
In order to verify the right ratio between metals ions, Mg and Al, were carried out EDX analyses, results (**Table 13**) show the right Mg/Al ratio for almost catalysts, it seems to be too low only HT-PMMA80.

	HT-PMMA127	HT-PMMA100	HT-PMMA90	HT-PMMA80
A.A. ratio Mg/Al	1,89	2,06	2,06	1,55

Table 13: EDX analysis on HT-PMMA materials to verify the right Mg/Al ratio.

XRD analysis, was tested the re-enactment ability, comparing the patterns obtained from the materials in each steps. The typical HTlc's pattern was recorded on each HT-PMMA before the calcinations process in order to identify the most intense diffraction peaks (**Graph 19**). The (00*l*) reflections are characterised by high intensities combined with a broad lineshapes indicating that the hydrotalcite has very small crystallite. The crystallites sizes were calculated from the (003) and (006) using the Debye-Scherrer equation:

$$\tau = \frac{0,89\lambda}{(\beta(\theta)\cos\theta)}$$



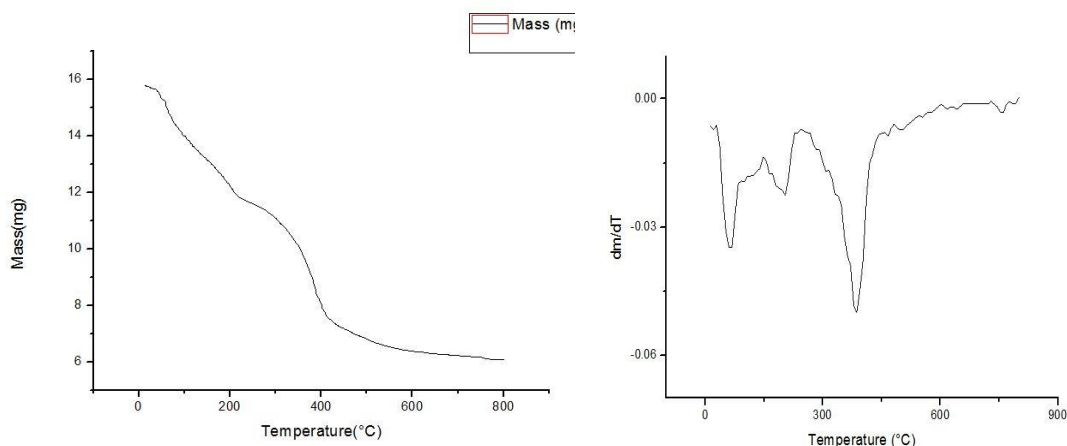
Graph 19: XRD trends of all HTlc materials before calcinations process.

This study allowed to carry out the calcinations process of HT-PMMA compounds using the same conditions used during the syntheses of the others materials, because for those, it is sure the total decomposition of the templating agent.

XRD analyses have been carried out in order to investigate the phase's composition of the new materials; on **Graph 19** it is possible observe the trends of all materials before the calcinations process. All show peaks at same 2θ value, meaning the similar diffraction interaction of x-rays with the scatterers atoms. The patterns show different relative intensities due by different crystallise level; for that, the templating agent plays an important role. When the template is PS, the peaks shape is enlarged (2θ = 25°), behaviour not observed when the templating agent is the PMMA; the mainly reason of these trends is accounted for the electron clouds of the scatterers atoms, affected by the surrounded atoms.

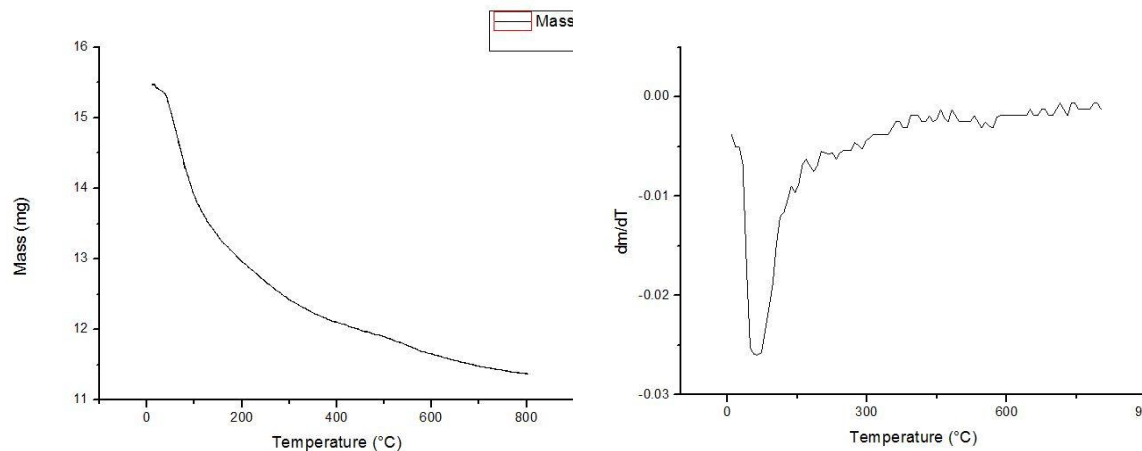
3.4.2 TGA/DGA, porosimetry analyses, SEM and TEM

TGA/DGA analyses were carried out to verify traces, due by the monomer, surfactant and initiator (**Graph 20**), before and after the thermal treatment. The thermogravimetric analyses on all the HT-PMMA materials show the same trends.



Graph 20: Thermogravimetric analysis of HT-PMMA material before the calcinations process (left).

Thermogravimetric analysis of HT-PMMA material; differential behaviour before calcinations (right).



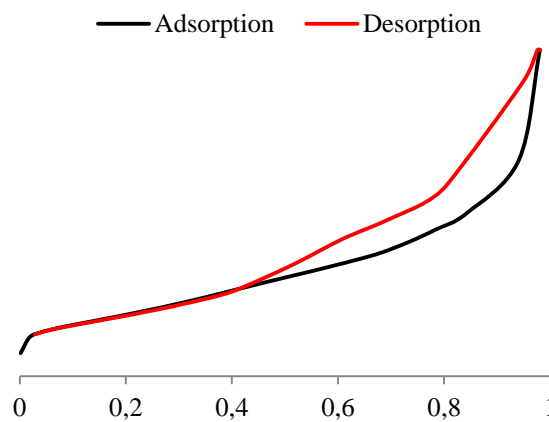
Graph 21: Thermogravimetric analysis of HT-PMMA material after the calcinations process(left).

Thermogravimetric analysis of HT-PMMA material after the calcinations process(right).

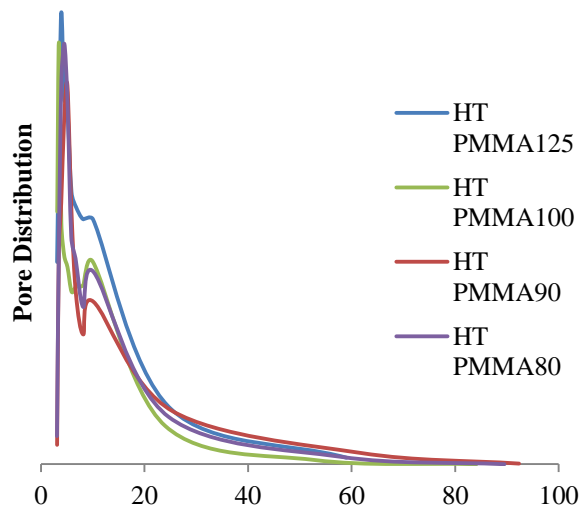
Before heat treatment (**Graph 20-right**), it is possible observe mass losses related to decomposition of the spheres of PMMA and water between 100 and 150 °C and the loss of carbonates near 350-400 °C. The peak relative to the loss of water (100°C) remains also after calcinations (**Graph 21-right**); similar results after the treatment have been obtained with CONV-HT and HT-PS (**Graph 15-16**). The mass loss (26,7%) is due to

the interlayer water, even if the decomposition temperature is close to that of MMA monomer, it is possible to reject the hypothesis that it is still trapped in the structure. The thermal treatment reaches temperatures above 300 ° C for which the monomer and the polymer are decomposed. These studies, allowed us to carry out the calcinations process as the one used for HT and HT-PS; the entire mass loss, indeed has got temperature, that is under the maximum of the reached temperature by the thermal process.

Porosimetry analyses were carried out to investigate the surface area values, pores volume and size for the new materials after thermal treatment (**Fig. 35-36**).



Graph 22: BET analysis on the HT-PMMA compound.



HT-PMMA125 HT-PMMA100 HT-PMMA90 HT-PMMA80

Surface Area (m²/g)	181	124	107	130
---------------------------------------	-----	-----	-----	-----

Pore Diameter (nm)	3,914	3,469	4,519	5,108
Pore Volume (cc/g)	0,422	0,286	0,378	0,354

Graph 23: BET/BJH analysis on the HT-PMMA compound.

Graph 22 shows the same trends of CONVHT and HT-PS: hysteresis behaviour between the adsorption and desorption, described by the BET model as an Isotherm IV type; on **Graph 23** is possible to observe the results obtained by BET/BJH analysis. From the analyses there are some values, which are not in the trend expected; an example is the surface area trend, which seems to not follow a particular scheme. One hypothesis may be due to polar, both attractive and repulsive, interactions between the polymer spheres and the aqueous solution, in which the precipitation occurs. Furthermore, it can be possible that, increasing the water amount during the synthesis of HTlc, the spheres aggregate forming flocculation. The problem of these groups of spheres is when the HT synthesis starts without their breakage; it is, indeed, no well dispersion and consequently, there is no ordered templated HT. Thus, during the research project, we have decided to work achieving a better activity comparison, with only one of the HT-PMMA synthesised: HT-PMMA100.

SEM and TEM analyses were conducted in order to verify the presence of a structural regularity from the templating agent (**Image 7-8**).

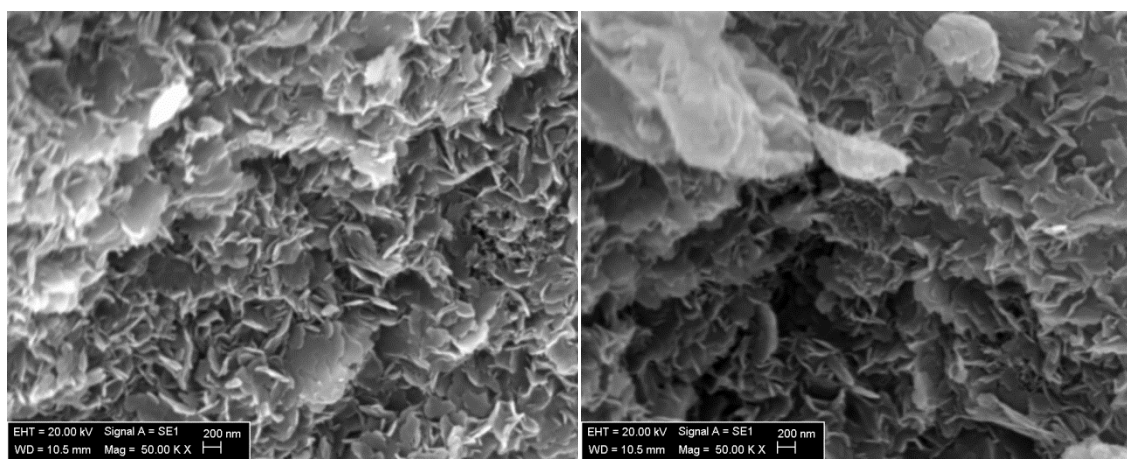


Image 7: SEM HT-PMMA100 with a different magnification(up- left /right).

Image 7: SEM HT-PMMA100 with a different magnification (down-left)

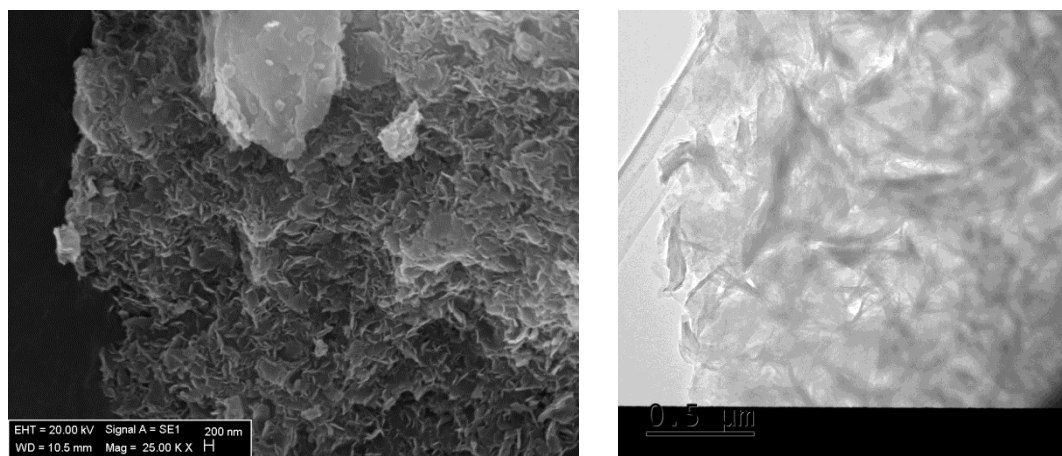


Image 8: TEM HT-PMMA100.

The results show the “sand roses” morphology characteristic of the hydrotalcite materials; the printing from template is lightly observable by the plates arrangement. TEM image reveals the disordered distribution of the pores. In order to investigate the base sites of the materials were carried out CO₂ titration analyses and results are shown on **Table 14**.

	CONV HT	HT-PMMA100	HT-PS280
Base sites (mmol/g)	0,11	0,074	0,051

Table 14: CO₂ titration analyses on each used catalyst.

According with XRD analyses, the attitude of CONV-HT to incorporate water, is higher than the HT-PS280, consequently is higher also reconstruction. CO₂ titrations were carried out in order to calculate the base sites number of CONVHT and HT-PS280, assuming a stoichiometry of one CO₂ molecule per base site, results are shown on **Table 14**.

3.5 Catalytic Transesterification

The materials activity CONVHT, HT-PS280 and HT-PMMA100, were tested on transesterification reaction, using triglyceride C4 and C8, methanol at 60 °C for different reaction times. As reported, in order to increase the TGC8 solubility in the reaction environment, we added butanol, 18,5 wt% respect to methanol. The kinetic study on TGC4 and TGC8 transesterification were performed both twice, with and without butanol, in order to study its influence on the reaction.

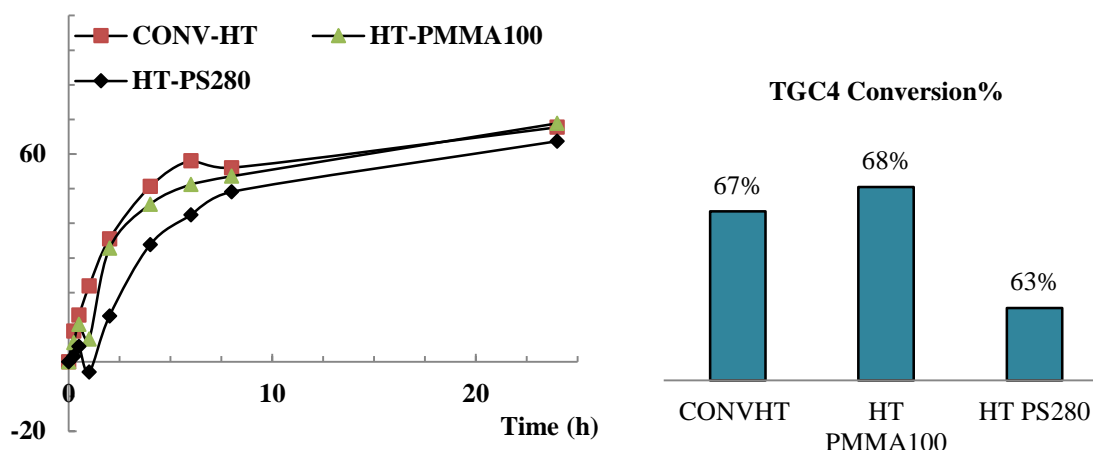


Figure 4: Transesterification reaction of TGC4 without butanol.

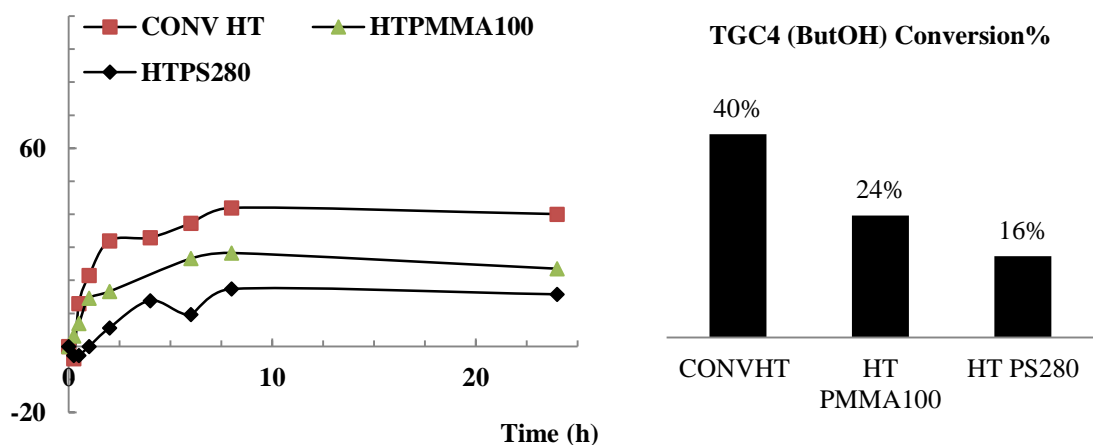


Figure 5: Transesterification reaction of TGC4 with butanol.

The TGC4 results are shown on **Figure 3-4/Table15**:

- CONV-HT and HT-PMMA100 have the best performance when the reaction occurs without butanol, obtaining 67% and 68% respectively of conversion after 24 hours; however, the one obtained with HT-PS280 is still comparable with those (63%). After 2 reaction hours, CONV-HT and HT-PMMA100 show similar trends 35% of TGC4 conversion (X%) for the first and 33% for the second meaning a similar initial rate value: $0,037 \text{ mmol}/\text{min}^{-1}$ (CONVHT) and $0,021 \text{ mmol}/\text{min}^{-1}$ (HT-PMMA100). Considering TOF value (min^{-1}) of both catalysts, we obtained the highest value ($6,69 \text{ min}^{-1}$) with CONV-HT catalyst (against $5,77 \text{ min}^{-1}$ with HT-PMMA100). Both performances are higher than the one obtained with HT-PS280. Using HT-PS280, we have the lowest performances as

conversion values (after 2 reaction hours) as initial rate and TOF value; for example, after 2 hours the TGC4 conversion is about 14%, as an half of the one obtained with the others catalyst and the TOF is $2,55 \text{ min}^{-1}$.

- When the reaction occurs with butanol (**Fig. 4**), the differences between catalysts become higher, showing, in each case, not only a decrease of final conversion but also a decrease of initial rate value (after 2h). In addition, the two catalysts, CONV-HT and HT-PMMA100, which in the previous case have occurred to similar values, now bring to different performance in the reaction environment. Considering the final conversion, we have about 40% for CONV-HT and 24% for HT-PMMA100; after 2h, X(TGC4)% with CONVHT is about 31% and it is about 16% with HT-PMMA100. Anyway the TOF value is higher with HT-PMMA100, $2,1 \text{ min}^{-1}$, than the one with CONV-HT($1,61 \text{ min}^{-1}$); that depends by the number of base sites on the surface of each catalyst. About HT-PS280 performance, we have also in this case the lowest values.

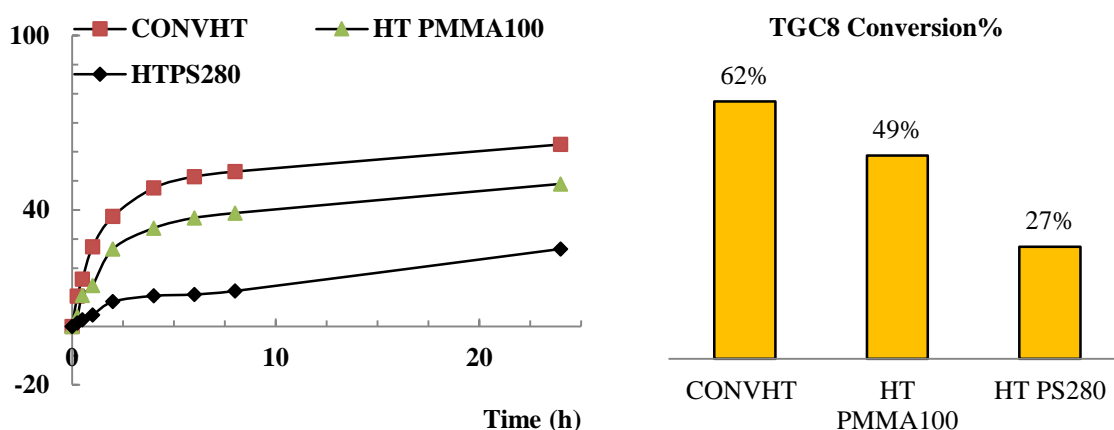


Figure 6: Transesterification reaction of TGC8 without butanol.

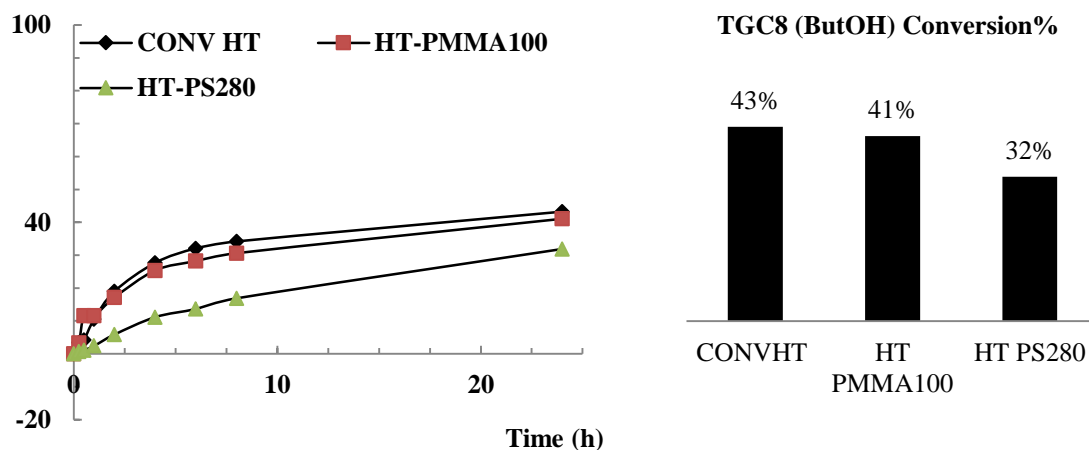


Figure 7: Transesterification reaction of TGC8 with butanol.

The TGC8 results are shown on **Figure 5-6/**Table 15:

- Using as reactant a longer chain triglyceride (TGC8) without butanol, catalysts show different behaviours: after 2 reaction hours, X% TGC8, is 38% with CONV-HT, 27% with HT-PMMA100 and about 9% with HT-PS280; after 24 reaction hours TGC8 conversion is 62% with CONV-HT, 49% with HT-PMMA100 and 27% with HT-PS280. Regarding the initial rate, calculated after 2 hours, CONV-HT has the highest value: 0,027 mmol/min, which is the same of HT-PMMA100, against 0,014 mmol/min of HT-PS. Considering the TOF, the highest value is the one of HT-PMMA100, 6,9 min⁻¹, followed by 5,63 min⁻¹ of HT-PS280 and last 4,9min⁻¹ of CONV-HT. We could suppose that the designed structured of the catalyst, even low, increase the TOF value also when the number of base sites is not high.
- When butanol is used (**Figure 6**), CONV-HT and HT-PMMA100 have almost same trend, both lower than the previous case; a similar consequence is shown when it is used HT-PS280 as catalyst. After 2 reaction hours, X% TGC8, is about 18% as with CONV-HT as with HT-PMMA100 and about 6% with HT-PS280; after 24 reaction hours TGC8 conversion is 43% with CONV-HT, 41% with HT-PMMA100 and 32% with HT-PS280. Regarding the initial rate, calculated after 2 hours, CONV-HT has the highest value 0,0059 mmol/min, which is almost the same of HT-PMMA100 (0,0053 mmol/min), against 0,0016 mmol/min of HT-PS280. Considering the TOF, the highest value is the one of HT-PMMA100, 1,43 min⁻¹, followed by 1,08 min⁻¹ of CONV-HT and last 0,65 min⁻¹ of HT-PS280.

	Initial Rate/ mmol min ⁻¹			TOF/ (min ⁻¹)		
	CONV	HT-	HT-	CONV	HT-	HT-PS280
	HT	PMMA100	PS280	HT	PMMA100	
TGC4	0,037	0,021	0,0065	6,69	5,77	2,55
TGC8	0,027	0,027	0,014	4,91	6,94	5,63
TGC4BUTOH	0,0089	0,0078	0,0022	1,62	2,11	0,84
TGC8/BUTOH	0,0059	0,0053	0,0016	1,08	1,43	0,65

Table 15: Reaction data for the triglyceride C4 and C8 transesterification with and without butanol.

4. DISCUSSIONS

New fascinating research's fields are growing during the last decade; they most of all are about bioenergy and biofuels. As we said, there are new generations of biofuel in the world's focus, but they need several years so that will be technologically relevant. In the present work, we tried to develop new catalysts, with ordered structures to apply in the transesterification reaction, at the moment, the main reaction to produce biodiesel. This project tries to increase the catalytic efficiency of transesterification reaction, designing a catalyst with a proper structure, thank to a templating agent.

4.1 HT, HT-PS and HT-PMMA characterisations

By the synthesis of HT-like compounds, used as catalyst for reaction, it can say that:

- From MP-AES and EDX analyses, it was possible verify the atomic ratio between two metals included in the structure. The analyses were carried out on conventional HT material and templated HTlcs with PS and PMMA. These tests are important also in order to make comparable the activity of catalysts in the reaction. Anyway, fluctuating values have been obtained in the range from 1,8 and 2,1; as well reported, this values are usual, and it may depend from the different area where the analysis is been carried out. As support of EDX analyses, conventional HT have been analysed with MP-AES instrument, that studies the entire mass of sample and not only a limited portion.
- By TGA/DGA it was possible estimate the purity of material after hydrothermal process; we compared the TGA and DGA graphs, and at which temperature it is observed the mass loss. Using templating agent, it is possible to some compound remain on the material surface. Hopefully, our tests have same results and trends, so we can consider the materials as the same material with the same component, remember, not the same structure.
- The hydro-treatment used wet nitrogen flow, obtained bubbling gas into water. By the tests, it seems to be relevant not its during time but the flow rate of gasses. However, with every material: HT, HT-PS280, HT-PS750 and brand HT-PMMA have same results, showing similar "memory effect". In order to reduce the time of the process and its entire synthesis, we can carry out the treatment for 24 hours.

- By porosimetry analysis, all the materials show a hysteresis behaviour associable to the BET model of IV Type. The higher surface area ($233\text{m}^2/\text{g}$) belongs to conventional HT compound, followed by HT-PMMA and at the end, HT-PS. In this list, the fall of surface area is due to size increasing of the templating agent. **Graph 14** shows trends linked to HT and HT-PS, it is clear, for both of them that as soon as higher the size of templant, higher will be pores volume and diameter.
- SEM analyses have been useful to verify the procedure and to test the right work of it. HTlc materials have the famous “sand roses” (**Image 1**), and, as well as reported, that is considered a proof of a correct synthesis. The same surface shape is observed on HT-PS (280 and 750) and HT-PMMA (100). On each of reported images, it is possible observe a sort of disposition of planes, more or less evident, depending from the templats’ size. For example, HT-PS750 even though has the typical HTlc’s morphology, it was not able to template the material structure during its growth. In the future, it can be useful trying to synthesise again HT-PS750, using the same obtained ratio between the size of particles (PS) and mass of hydrotalcite of HT-PS280. However, when the analysis is carried out on HT-PMMA, it is possible observe a sort of rearrangement of planes. These arrangement follow a “sand roses” shape, and templating action is observable by the growth of planes is round the polymer’s spheres, such as they worked only as a guide and not as templating agents. An option to make the reaction more efficient, may be, as said above, changing the ratio of masses used.
- CO_2 titration analyses are reported on **Table 14**; it is possible observe the relationship between, surface area and base sites: indeed, decreasing the surface area, the number of base sites (from HT, through HT-PMMA100, ending with HT-PS280), is rightly reduced also.

4.2 PMMA characterisations

The synthesis of PMMA as nano-particles is not easy; there are several disadvantages, which increase the number of difficulties of reaction, such as the necessity to work under inert atmosphere and with no light, in order to reduce the chance to have unwanted reactions. At the same time, it is possible obtain a wide range of size if the condition are all respected. By the study, we can say:

- On one hand, decreasing water volume it is possible reduce the size distribution and decrease diameters. Keeping SDS as constant, the particles diameter; at the same condition, it is observed a larger size distribution, when volume increase.
- On the other hand, increasing the SDS amount it is possible obtaine smaller diameters.

Furthermore, after reaction, the breakage of the colloidal solution may became a key point to develop a good method and to obtain PMMA as solid spheres. One option may be to use harder centrifugal condition. A good result is reported on SEM image, where the distribution of sizes is acceptable. Anyway, as we tested, vacuum techniques lead the nano-spehers to transform itself into an amorphous glassy material.

4.3 Tranesterification Reaction

The kinetic study on TGC4 and TGC8 transesterification were performed both twice, with and without butanol, in order to study its influence on the reaction, using as catalysts: conventional HT, HT-PS280 and HT-PMMA100.:

- It is possible assume that with triglycerides with short chain as C4, the ordered structure is not significant; decreasing the surface of catalyst we have lower activity, so that the conversion. Unfortunately the reduction of surface area is caused by the using of a templating agent, PMMA(100 nm) to 125m²/g and PS280 (280 nm) to 80 m²/g. Indeed best performance are with conventional HT, by which it reached the 67% of conversion.
- When there is no butanol into the reaction environment, catalysts performances of TGC4 conversion are comparable only after 24h. Using butanol, conversion's results decrease meanly due to catalyst deactivation caused by poisoning. Usually, a second alcohol is useful to increase the solubility of each reactant to the solution, and it avoids the formation of a three phase's system. TGC4 is almost soluble into the liquid phase. Anyway, we tested the butanol's influence to the system in order to have a better view of the reaction.
- Using a longer chain triglyceride (TGC8) without butanol, catalysts show different conversions: 62% with CONV-HT, 49% with HT-PMMA100 and 27% with HT-PS280. Also in these cases, as higher is the surface area of catalysts as higher is the conversion. Designed structures of the catalyst, such as HT-PMMA may affect only the initial rate estimated on the first 2 reaction hours.

- Using buthanol with TGC8, the consequences of conversion loss are less evident, probably due to a higher solubility of the reactant, thus a lower poisoning of catalyst.

5. CONCLUSIONS

More test need to be done, in order to verify the catalyst activity with longer chain TG. By these test may be possible understand clearer the role on the reaction of catalyst's structure. At the same time, more tests can be done carrying out reaction with higher temperature, reaching higher conversion and rate. New tests need to be done to improve micro and meso porosity, and it may be possible, by studying the right ratio between the diameter of spheres templant and the mass of each HTlc to be synthesised. Moreover, new tests can use a different kind of catalyst, always HTlc but, which has or both physic and chemical promoters, or a different kind of trivalent metal, or easily changing the Mg/Al ratio.

6. ACKNOWLEDGEMENT

I would like to thank my supervisor Prof. Fabrizio Cavani for his patience over the last year.

I would like also to thank Dr. Karen Wilson, dear supervisor member of the School of Chemistry at Cardiff University.

I wish to express my sincere thank to the Department of Industrial Chemistry of the School of Science, University of Bologna, giving me the chance to take apart at the project "Tesi all'Estero", and supporting over the six months carried working at the School of Chemistry of Cardiff University.

7. REFERENCES

- Bastiani, R. et al., 2004. Influence of thermal treatments on the basic and catalytic properties of Mg,Al-mixed oxides derived from hydrotalcites. *Brazilian Journal of Chemical Engineering*, 21(2), pp. 193-202.
- Bellotto, M., Rebours, B., Clause, O. & Lynch, J., 1996. hydrotalcite Decomposition Mechanism: A Clue to the Structure and Reactivity of Spinel-like Mixed Oxides. *J. Phys. Chem.*, Issue 100, pp. 8535-8542.
- Biofuel.org, 2010. *Biofuels - The fuel of the future*. Available at: <http://biofuel.org.uk/>
- Biomass Power Association, 2009. *Biomass Energy in North America Opportunities and Challenges*. s.l., IEA Bioenergy ExCO72.
- Bolognini, M. et al., 2003. Mg/Al mixed oxides prepared by coprecipitation and sol-gel routes: a comparison of their physico-chemical features and performances in m-cresol methylation. *Microporous and Mesoporous Materials*, Issue 66, pp. 77-89.
- Cavani, F., Centi, G., Perathoner, S. & Trifirò, F., 2009. *Sustainable Industrial Chemistry*. s.l.:s.n.
- Cavani, F., Trifirò, F. & Vaccari, A., 1991. hydrotalcite-type anionic clays: preparation, properties and applications. *Catalysis Today*, Volume 11, pp. 173-301.
- D.G. Cantrell, L. G. A. L. a. K. W., 2005. Structure-reactivity correlations in MgAl hydrotalcite catalysts for biodiesel synthesis. Issue 287, pp. 183-190.
- E. Géraud, V. P. a. F. L., 2006. Synthesis and characterization of macroporous MgAl LDH using polystyrene spheres as template. In: s.l.:ELSEVIER, pp. 903-908.
- Gao, Y., Chapin, G. & Liang, Y., 2012. Algae biodiesel - a feasibility report. *Chemistry Central Journal*, Volume 6.
- Géraud, E., Prévot, V., Ghanbaja, J. & Leroux, F., 2005. Macroscopically Ordered Hydrotalcite-type Materials Using Self-Assembled Colloidal Crystal Template. *Chem. Mater.*, 23 12, Issue 18, pp. 238-240.

Hibino, T. & Tsunashima, A., 1997. Formation of spinel from a hydrotalcite-like compound at low temperature: reaction between edges of crystallites. *Clays and Clay Minerals*, 45(6), pp. 842-853.

Hibino, T., Yamashita, Y., Kosuge, K. & Tsunashima, A., 1995. *Decarbonation behavior of Mg-Al-CO₃ hydrotalcite like compounds during heat treatment.*

IEA Bioenergy, 2011. *Environmental Sustainability of Biomass*, s.l.: s.n.

IEA Bioenergy, 2012. *Annual Report 2012*, s.l.: IEA Bioenergy.

International Energy Agency, 2007. *Good Practice Guidelines. Bioenergy Project Development & Biomass Supply*, Paris Cedex: IEA Publications.

Klemes, J. J., Varbanov, P. S. & Lam, H. L., 2011. *Chemical Engineering Transactions*, Volume 25.

Kosuge, Y., Hibino, T. & Tsunashima, A., 1996. Synthesis of carbon-hydrotalcite complex and its thermal degradation behavior. *Clays Clay Miner*, Volume 44, pp. 151-152.

Lotero, E. et al., 2005. Synthesis of Biodiesel via Acid Catalysis. *Ind. Eng. Chem. Res.*, Volume 44, pp. 5353-5363.

Melero, J. A., Morales, J. I. & Morales, G., 2009. Heterogeneous acid catalysts for biodiesel production: current status and future challenges. *Green Chemistry*, 6th July, Issue 11, pp. 1285-1308.

Millange, F., Walton, R. I. & O'Hare, D., 2000. Time-resolved in situ X-ray diffraction study of the liquid-phase reconstruction of Mg-Al-carbonate hydrotalcite-like compounds. *J. Mater. Chem.*, Issue 10, pp. 1713-1720.

Miller, J. B. & Ko, E. I., 1997. Control of mixed oxide textural and acid properties by sol-gel method. *Catalysis Today*, 35(3), pp. 269-292.

Mizoshita, N., Tani, T. & Inagaki, S., 2011. Syntheses, properties and applications of periodic mesoporous organosilicas prepared from bridged organosilane precursors. *Chem. Soc. Rev.*, Issue 40, pp. 789-800.

Morell, J. et al., 2006. Synthesis and Characterisation of highly ordered bifunctional aromatic periodic mesoporous organosilicas with different pore sizes. *Journal Of Materials Chemistry*, Issue 16, pp. 2809-2818.

Norakankorn, C., Pan, Q., Rempel, G. & Kiatkamjornwong, S., 2007. Synthesis of Poly(methyl methacrylate) Nanoparticles Initiated by 2,2'-Azobisobutyronitrile viaa Differential Microemulsion Polymerization. Volume 28, pp. 1029-1033.

NREL, 2003. Production of biodiesel from multiple feedstock and properties of biodiesel and biodiesel/diesel blends. Final report.

Perlack, R. D. et al., 2005. *Biomass as Feedstock for a Bioenergy and Bioproducts Industry: The Technical Feasibility of a Billion-Ton Annual Supply*, s.l.: s.n.

Rao, P. V., Clarke, S. & Brown, R., 2010. Influence of iodine value on combustion and NOx emission characteristics of a DI diesel engine. *Chemeca 2010: The 40th Australasian Chemical Engineering Conference*.

Riahi, K. et al., 2004. Technological Learning for Carbon Capture and Sequestration Technologies. *Energy Economics*, 4(26), pp. 539-564.

Saikia, P. J., Lee, J. M., Lee, B. H. & Choe, S., 2007. Reversible Addition Fragmentation Chain Transfer Mediated Dispersion Polymerization of Styrene. *Macromol. Symp.*, Issue 248, pp. 249-258.

Schuchardt, U., Sercheli, R. & Vargas, R. M., 1998. Transesterification of VEgetable Oils: a Reiew. *J. Braz. Chem. Soc.*, 9(1), pp. 199-210.

Shen, J., Kobe, J. K., Chen, Y. & Dumesic, J., 1994. Synthesis and Surface Acid/Base Properties of Magnesium-Aluminum Mixed Oxides Obtained frlm Hydrotalcites. *Langmuir*, Issue 10, pp. 3902-3908.

Shuit, S. H. et al., 2013. *Evolution towards the utilisation of functionalised carbon nanotubes as a new generation catalyst support in biodiesel production: an overview*, s.l.: RSC Advances.

Somorjai, G. A., 1994. *Introduction to surface chemistry and catalysis*. New York, NY: John Wiley & Sons, Inc..

Alma Mater Studiorum – Università di Bologna

Vinogradov, V. V., Vinogradov, A. V. & Agafonov, A. V., s.d. Template-assisted sol-gel approach to synthesize new prospective alumina based catalysts.

Wijffels, R. H. & Barbosa, M. J., 2010. An Outlook on Microalgal Biofuel. *Science*, Volume 329.

Wilson, E. J., Friedmann, S. J. & Pollak, M. F., 2007. Research for Deployment: Incorporating Risk, Regulation, and Liability for Carbon capture and Sequestration. *Environmental Science & Technology*, 41(17).

Woodford, J. J., Dacquin, J.-P., Wilson, K. & Lee, A. F., 2012. Better by design: nanoengineered macroporous hydrotalcites for enhanced catalytic biodiesel production. *The Royal Society*, Volume 5.

Xu, S. et al., 2011. Engineered morphologies of layered double hydroxide nanoarchitected shell microspheres and their calcined products. *Chemical Engineering Science*, Issue 66, pp. 2157-2163.